AD_____

Award Number: DAMD17-03-1-0383

TITLE: The Effects of Deregulated Cyclin Expression in Mitosis. A Role in Breast Tumorigenesis

PRINCIPAL INVESTIGATOR: Jamie M. Keck, Ph.D.
Steven I. Reed, Ph.D.

CONTRACTING ORGANIZATION: The Scripps Research Institute
La Jolla, California 92037

REPORT DATE: May 2006

TYPE OF REPORT: Annual Summary

PREPARED FOR: U.S. Army Medical Research and Materiel Command
Fort Detrick, Maryland 21702-5012

REPORT DOCUMENTATION PAGE

Form Approved
OMB No. 0704-0188

1. REPORT DATE *(DD-MM-YYYY)*	**2. REPORT TYPE**	**3. DATES COVERED** *(From - To)*
01-05-2006	Annual Summary	1 May 2003 – 30 Apr 2006

4. TITLE AND SUBTITLE

The Effects of Deregulated Cyclin Expression in Mitosis. A Role in Breast Tumorigenesis

5a. CONTRACT NUMBER

5b. GRANT NUMBER
DAMD17-03-1-0383

5c. PROGRAM ELEMENT NUMBER

6. AUTHOR(S)

Jamie M. Keck, Ph.D. and Steven I. Reed, Ph.D.

E-Mail: jamiekeck@gmail.com

5d. PROJECT NUMBER

5e. TASK NUMBER

5f. WORK UNIT NUMBER

7. PERFORMING ORGANIZATION NAME(S) AND ADDRESS(ES)

The Scripps Research Institute
La Jolla, California 92037

8. PERFORMING ORGANIZATION REPORT NUMBER

9. SPONSORING / MONITORING AGENCY NAME(S) AND ADDRESS(ES)
U.S. Army Medical Research and Materiel Command
Fort Detrick, Maryland 21702-5012

10. SPONSOR/MONITOR'S ACRONYM(S)

11. SPONSOR/MONITOR'S REPORT NUMBER(S)

12. DISTRIBUTION / AVAILABILITY STATEMENT
Approved for Public Release; Distribution Unlimited

13. SUPPLEMENTARY NOTES

14. ABSTRACT

The purpose of this project is to study the effects of constitutive cyclin E expression on mitotic division and to better understand the mechanisms through which cyclin E leads to chromosome instability. Cyclin E functions to promote the G1/S phase transition and centrosome duplication; however, deregulation of cyclin E expression in cell culture results in premature entry into S phase and induces a moderate level of chromosome instability. We show that deregulated cyclin E can directly interfere with mitotic division leading to chromosome instability. Cells delay in late stages of prometaphase prior to complete alignment of chromosomes at the metaphase plate. In some cases, cells fail to divide chromosomes and instead return to interphase, resulting in polyploidy. In this third year of funding, I have completed the final goal of the project to determine the mechanism by which cyclin E delays mitosis. Cyclin E was found to inhibit the anaphase promoting complex (APC) ubiquitin ligase by inhibiting the specificity subunit, Cdh1, through a kinase-dependent mechanism. This inhibition led to significant accumulation of APC-Cdh1 substrates, cyclin B1, Cdc20, and securin. Furthermore, reducing Cdh1 in cells by RNAi mimics the protein accumulation and mitotic delay phenotypes observed upon cyclin E deregulation.

15. SUBJECT TERMS
Cyclin E, chromosome instability, cell cycle, mitosis, centrosome

16. SECURITY CLASSIFICATION OF:			**17. LIMITATION OF ABSTRACT**	**18. NUMBER OF PAGES**	**19a. NAME OF RESPONSIBLE PERSON**
a. REPORT	**b. ABSTRACT**	**c. THIS PAGE**			USAMRMC
U	U	U	UU	47	**19b. TELEPHONE NUMBER** *(include area code)*

Table of Contents

Introduction

Deregulation of the cell cycle and genomic instability are hallmarks of tumorigenesis. The cell cycle is regulated through the periodic expression of cyclins. Cyclin E expression is normally limited to the G1/S boundary where it promotes initiation of DNA replication and centrosome duplication. Deregulated cyclin E in cell culture results in a premature but elongated S phase (Resnitzky et al., 1994), and chromosome instability following constitutive cyclin E expression (Spruck et al., 1999). In cyclin E transgenic mice, tumor incidence is increased , especially with expression of a hyperstable cyclin E mutant (Bortner and Rosenberg, 1997; Smith et al., 2006). The purpose of this study was to investigate the effects of constitutive cyclin E expression on mitotic division and to ultimately identify the mechanism through which cyclin E leads to chromosome instability. We show that one pathway leading to genomic instability might be through a delay in mitosis and failure to properly segregated chromosomes. This report describes the results found during this study, including the deregulation of the cell cycle following constitutive cyclin E expression, observations of a mitotic delay in cyclin E expressing cells, the accumulation of mitotic regulatory proteins up to and during mitosis, and the inhibition of the APC-Cdh1 complex by deregulated cyclin E.

Body

Task 1 - completed in first year: Characterization of cells transduced with cyclin E retrovirus and adenovirus (1-9 months)

This task was completed in the first and second reports. See attached paper in the appendix, Figure 1, page 14. In summary, we constructed both a retrovirus and adenovirus to constitutively express cyclin E in cultured cells. Cell cycle analysis was done using flow cytometry and immunofluorescence. An accumulation of cells in S phase and in G2/M phases were observed with flow cytometry. Next, we used immunofluorescence to distinguish whether cells were accumulating in G2 or in mitosis (see appendix, Figure 2a, page 17). A decrease of G2 cells with cyclin E deregulation was observed; therefore, we concluded that the accumulation was due to a delay in mitosis.

Task 2 – completed in first and second years: Observation of aberrant mitoses with fixed and live cell microscopy (Months 8-17)

This task was completed in the first and second reports. See attached paper in the appendix, Figures 2b and 3, pages 17 and 19). In summary, immunofluorescence was used to count fixed cells in mitosis. We characterized six phases of mitosis, Prophase, Prometaphase, Unaligned metaphase, Metaphase, Anaphase-telophase, and Cytokinesis. Cells with deregulated cyclin E expression accumulated in early stages of mitosis, specifically prometaphase and unaligned metaphase, compared to controls. This result was confirmed using live-cell microscopy to observe chromosome dynamics in real-

time. Cells expressing cyclin E were found to delay before complete alignment of chromosomes on the metaphase plate, confirming the previous result using fixed cells. In addition, we observed other mitotic defects such as a failure to align chromosomes completely prior to anaphase and a complete failure to divide chromosomes.

Task 3: (completed in second year) - Quantification of centrosomes in cells transduced with cyclin E (Months 17-23)

This task was completed in the second report. In the end, this was not a vital experiment to our findings so it is not discussed in the attached paper. We used immunofluorescence to count centrosomes in cells with cyclin E overexpression and found an 8% increase in the number of cells with greater than 2 centrosomes. Because cells contained 4 centrosomes, rather than 2, this confirmed our results that cells were failing mitosis and were accumulating centrosomes.

Task 4: (completed in third year) - Investigate targets of cyclin E/Cdk2 phosphorylation in mitosis (Months 24-36)

The task of investigating the mechanism by which cyclin E leads to a mitotic delay was the most crucial objective in this project. In the midterm report, anaphase promoting complex (APC) substrates were shown to accumulate up to and through mitosis due to increased protein stability. See appendix, Figure 5, page 23).

The next objective was to determine the cause of the APC substrate accumulation. In the midterm report, increased levels of BubR1 protein, an inhibitor the APC-Cdc20 complex in metaphase, was proposed to be the main cause of the mitotic delay, as reducing BubR1 by RNAi could override phenotypes due to cyclin E deregulation. However, we were unable to recapitulate the mitotic delay and protein accumulation by ectopically overexpressing BubR1 by adenoviral transduction. Most likely, reducing BubR1 simply floods the cell with active APC-Cdc20 complexes, essentially releasing the spindle checkpoint and forcing progression into anaphase.

A great amount of evidence now points toward Cdh1 as the direct substrate of cyclin E phosphorylation responsible for inhibiting the APC ubiquitin ligase. Cdh1 is normally inhibited through phosphorylation by cyclin A-Cdk2 during S and G2 phases. We demonstrate that deregulated cyclin E is able to bind and phosphorylate Cdh1 in vitro, leading to a further inhibition of the APC-Cdh1 complex (see appendix Figure 6, page 26). Also, cyclin E-Cdk2 phosphorylation of Cdh1 leads to direct inhibition of APC ubiquitin ligase activity in vitro (see appendix Figure 7, page 28). Furthermore, we show that reducing Cdh1 using siRNA can mimic APC substrate accumulation and the early mitotic delay (see appendix, Figure 8, page 29). Finally, the APC-Cdh1 substrates most relevant to the phenotypes caused by cyclin E deregulation are shown to be both cyclin B1 and securin (see appendix, Figure 9, page 32).

Key Research Accomplishments

- Determined the mechanism by which cyclin E deregulation leads to mitotic protein accumulation and early mitotic delays
- Demonstrated binding and phosphorylation of Cdh1 by cyclin E-Cdk2 in vitro
- Showed direct inhibition of the APC-Cdh1 ubiquitin ligase by cyclin E-Cdk2 in vitro
- Tested proposed mechanism by reducing Cdh1 in vivo using RNAi and measuring protein accumulation and mitotic progression

Reportable Outcomes

- Keck J. April 2005. Oral presentation: The Effect of Deregulated Cyclin E on Mitosis. The American Association of Cancer Research (AACR) Annual Meeting, Anaheim, CA. Awarded a Scholar in-training fellowship for travels.
- Keck J. June 2005. Poster presentation: The Effects of Cyclin E on Mitosis. DOD Breast Cancer Research Meeting, Philadelphia, PA
- Jamie M. Keck, Donato Tedesco, Matthew K. Summers, Peter K. Jackson, and Steven I. Reed. *Cyclin E deregulation impairs progression through mitosis by inhibiting* APC^{Cdh1}. Submitted to Journal of Cell Biology. August 2006.

Conclusions

During this final year of funding, I completed all goals set for this proposed project. In summary, we now have evidence that one important mechanism through which cyclin E deregulation leads to genomic instability is through the inhibition of APC-Cdh1 up to and during mitosis, causing accumulation of mitotic regulators and delays in mitosis. At times, mitotic division completely fails resulting in polyploid cells containing double the amount of DNA and centrosomes, thus explaining how cyclin E deregulation induces chromosome instability.

References

Bortner, D.M., and M.P. Rosenberg. 1997. Induction of Mammary Gland Hyperplasia and Carcinomas in Transgenic Mice Expressing Human Cyclin E. *Mol. and Cell. Biol.* 17:453-459.

Resnitzky, D., M. Gossen, H. Bujard, and S.I. Reed. 1994. Acceleration of the G1/S phase transition by expression of cyclins D1 and E with an inducible system. *Mol Cell Biol*. 14:1669-79.

Smith, A.P., M. Henze, J.A. Lee, K.G. Osborn, J.M. Keck, D. Tedesco, D.M. Bortner, M.P. Rosenberg, and S.I. Reed. 2006. Deregulated cyclin E promotes p53 loss of heterozygosity and tumorigenesis in the mouse mammary gland. *Oncogene*.

Spruck, C.H., K.-A. Won, and S.I. Reed. 1999. Deregulated cyclin E induces chromosome instability. *Science*. 401:297-300.

Appendix

Cyclin E deregulation impairs progression through mitosis by inhibiting APC^{Cdh1}.

Jamie M. Keck[1], Donato Tedesco[1,3], Matthew K. Summers[2,4], Peter K. Jackson[2,4] and Steven I. Reed[1*]

[1]Department of Molecular Biology, The Scripps Research Institute, La Jolla, CA 92037

[2] Department of Pathology, Stanford University School of Medicine, Stanford, CA 94305

[3] Present Address: Berlex, Inc., 2600 Hilltop Drive, Richmond, CA 94806

[4] Present Address: Genentec, Inc., One DNA Way, South San Francisco, CA 94080-4990

[*] Correspondence: sreed@scripps.edu

Running title: Cyclin E deregulation impairs mitosis

Abstract

Deregulation of cyclin E, an activator of cyclin-dependent kinase 2 (Cdk2), has been linked to human cancer. In cell culture models, forced expression of cyclin E leads to aneuploidy and polyploidy, consistent with a direct role of cyclin E deregulation in tumorigenesis. In the current study, we show that deregulated expression of cyclin E has a direct effect on mitotic progression. Specifically cells delay in latter stages of prometaphase prior to complete alignment of chromosomes at the metaphase plate. In some cases, such cells fail to divide chromosomes and instead return to interphase, resulting in polyploidy. In others, cells proceed to anaphase without complete alignment of chromosomes. From a mechanistic perspective, these phenotypes can be explained by an ability of deregulated cyclin E to inhibit residual APC^{Cdh1} activity that persists as cells progress up to and through the early stages of mitosis. Such inhibition results in abnormal accumulation of APC^{Cdh1} substrates as cells enter mitosis. We show further that accumulation of securin and cyclin B1, in particular, can account for the cyclin E-mediated mitotic phenotype in that partial knockdown of these proteins by RNAi restores normal mitotic progression under conditions of cyclin E deregulation.

Introduction

Cyclin E, an activator of cyclin-dependent kinase 2 (Cdk2), accumulates at the G1-S boundary of the cell cycle where it stimulates functions associated with entry into and progression through S phase (Ekholm and Reed, 2000; Ohtsubo et al., 1995 ; Resnitzky et al., 1994; Sauer and Lehner, 1995). Normally, cyclin E levels, and presumably cyclin E-associated Cdk2 kinase activity, are tightly regulated so that peak activity occurs only for a short interval near the G1-S boundary (Ekholm and Reed, 2000). This is accomplished primarily by periodic E2F-dependent transcription of cyclin E during late G1 phase (Dulic et al., 1992; Koff et al., 1991), and its subsequent phosphorylation-dependent ubiquitin-mediated proteolysis in S phase when cyclin E-Cdk2 complexes become active (Strohmaier et al., 2001). Cyclin E expression and activation of Cdk2 at the G1-S boundary are compatible with the known roles of cyclin E in promotion of replication-associated functions (Arata et al., 2000; Ekholm-Reed et al., 2004a; Geng et al., 2003; Mailand and Diffley, 2005).

Deregulation of cyclin E expression has been observed in a broad spectrum of human malignancies, suggesting that proper regulation of cyclin E is important for preservation of normal cellular functions (Ekholm-Reed et al., 2004b; Erlandsson et al., 2003; Keyomarsi et al., 1995; Sandhu and Slingerland, 2000; Spruck et al., 2002). Under such circumstances, cyclin E is often expressed at levels higher than those observed in normal tissues, but also the periodic expression at the G1-S boundary is frequently lost, with cyclin E levels maintained throughout the cell cycle. This can occur through a single mutation in Cdc4 (also known as Fbw7), the F-box component of an SCF ubiquitin ligase that targets cyclin E for ubiquitin-mediated degradation (Rajagopalan et al., 2004; Spruck et al., 2002; Strohmaier et al., 2001). Furthermore, deregulation of cyclin E in some cancers has been associated with aggressive disease and poor outcome (Dutta et al., 1995; Erlanson and Landberg, 2001; Keyomarsi et al., 2002; Nielsen et al., 1998; Porter et al., 1997). A direct causal link between between cyclin E deregulation and tumorigenesis is supported by a transgenic mouse model where ectopic expression of

cyclin E in the mammary epithelium induces mammary carcinogenesis (Bortner and Rosenberg, 1997; Smith et al., 2006).

The basis for cyclin E-induced tumorigenesis remains controversial. Because cyclin E, by virtue of its ability to activate Cdk2, is a positive regulator of the cell cycle, it has been proposed that the role of cyclin E in tumorigenesis is to stimulate cellular proliferation (Geng et al., 2003). This is consistent with the role of cyclin E-Cdk2 in phosphorylating and inactivating the retinoblastoma protein Rb, a negative regulator of proliferation (Harbour et al., 1999; Lukas et al., 1997; Zhang et al., 1999). Furthermore, ectoptic expression of cyclin E was shown to drive cultured cells from G1 into S phase with accelerated kinetics (Ohtsubo and Roberts, 1993; Resnitzky et al., 1994). However, in these studies the overall rate of proliferation was not altered, arguing against a direct link between cyclin E deregulation and increased proliferation in the context of tumorigenesis. On the other hand, cyclin E-mediated mammary hyperplasia was observed in mice carrying a mammary epithelium-specific cyclin E transgene, consistent with a link between cyclin E deregulation and cellular proliferation in vivo (Bortner and Rosenberg, 1997).

An alternative view of the role of cyclin E deregulation in tumorigenesis comes from studies of genomic instability. In cultured non-transformed cells, deregulation of cyclin E expression led to both chromosome instability and polyploidy (Spruck et al., 1999). Chromosome instability was a relatively infrequent event under moderate levels of cyclin E overexpression but was manifest reproducibly as both chromosome losses and gains, suggesting non-disjunction or other mitotic aberrations as possible mechanisms. Polyploidy was a more frequent event that was easily scorable under the experimental conditions. Polyploid cells, themselves unstable, can readily give rise to aneuploidy (Thiagalingam et al., 2000). Cyclin E deregulation in a tissue culture model has also been associated with the formation of micronuclei, suggestive of the generation of aneuploid cells (Rajagopalan et al., 2004). Genomic instability in the forms of both chromosome instability and polyploidy, leading to aneuploidy, could easily explain the link between cyclin E deregulation and tumorigenesis.

Genomic instability has been shown to promote tumorigenesis on a number of levels, most notably by facilitating loss of heterozygosity at tumor suppressor loci and amplification of oncogenes (Thiagalingam et al., 2000). Consistent with this interpretation, early loss of heterozygosity of the tumor suppressor gene encoding p53 was observed in the mouse mammary cyclin E transgenic model (Smith et al., 2006). Importantly, both aneuploidy and polyploidy have been observed in human tumors where cyclin E is deregulated (Hubalek et al., 2004).

In terms of the mechanism whereby cyclin E deregulation promotes genomic instability, cell cycle analysis has provided a number of clues. Early studies indicated that ectopic expression of cyclin E, although accelerating entry into S phase caused a significant prolongation of S phase (Ohtsubo and Roberts, 1993; Resnitzky et al., 1994). A more recent analysis revealed that deregulation of cyclin E expression specifically impairs assembly of pre-replication complexes upon mitotic exit, leading to slow and inefficient DNA replication, and most likely replicative stress (Ekholm-Reed et al., 2004a). It is easy to envisage how replication defects can lead to genomic instability. In another study where the cyclin E-targeting F-box protein Cdc4 was mutated in cultured cells, impairing cyclin E turnover, mitotic aberrations in some cells were observed by time-lapse videomicroscopy (Rajagopalan et al., 2004). However, this study could not distinguish between direct effects on mitosis and indirect effects accruing as a result of replicative stress, and since SCF^{Cdc4} also targets other cellular regulatory proteins, the effects could not be definitively attributed to cyclin E deregulation.

In the current study, we investigate whether cyclin E deregulation can have a direct impact on the progression through, and the quality of, mitosis. By expressing cyclin E in a manner that precludes effects on pre-replication complex assembly, we demonstrate that deregulation of cyclin E expression both delays progression through early phases of mitosis and causes mitosis to be executed aberrantly in many cells. Furthermore, we demonstrate that these effects are mediated by the direct action of cyclin E-Cdk2 on protein complexes that regulate mitotic progression.

Results

Deregulating cyclin E expression in cultured cells.

To study the effects of cyclin E deregulation, recombinant retroviruses and adenoviruses (Ekholm-Reed et al., 2004a) were engineered to efficiently deregulate cyclin E expression in cultured cells. The retrovirus was used to deliver a hyperstable form of cyclin E (cyclin E T380A) for long-term, stable expression. Mutation of the cyclin E phosphodegron at T380 severely impairs its ubiquitin-mediated degradation (Clurman et al., 1996; Won and Reed, 1996; Ye et al., 2004). Figure 1a shows immunofluorescence images comparing cyclin E expression in hTERT-immortalized mammary epithelial (IME) cells stably transduced with the cyclin E retrovirus (retro CyE) compared to cells transduced with empty-vector control retrovirus (retro EV Cont). Compared to control cells, cyclin E expression is upregulated and deregulated with respect to the cell cycle in cells transduced with retro CyE.

To study acute effects of cyclin E deregulation, a recombinant adenovirus expressing wild-type (WT) cyclin E from the constitutive CMV promoter was constructed (Ekholm-Reed et al., 2004a). As shown by Western blot (Figure 1b), KB cells 24 hours after transduction with cyclin E adenovirus (ad Cyclin E) have increased cyclin E expression compared to cells transduced with an empty-vector control adenovirus (ad EV Cont).

Cyclin E-Cdk2 kinase activity is normally restricted to late G1 phase and early S phase. To confirm that cyclin E overexpression resulted in the deregulation of cyclin E-Cdk2 kinase activity with respect to the cell cycle, kinase assays were performed on extracts from mitotic cells, where cyclin E is not normally expressed. To enrich for cells in mitosis, KB cells were synchronized using a single thymidine block at the G1/S boundary and then released for 8 hours into nocodazole (see Fig. 5a). As measured by ability of cyclin E immunoprecipitates to phosphorylate histone H1, cyclin E-Cdk2 kinase activity was detectable well above background in mitotically-enriched extracts following transduction with the cyclin E expressing adenovirus (Figure 1c).

Cyclin E induces genomic instability and cell cycle delays

Cyclin E deregulation was previously shown to induce genomic instability in a non-transformed human breast epithelial cell line and in rat fibroblasts (Spruck et al., 1999). Chromosome painting was used to further assess the types of genomic instability induced by cyclin E deregulation using an immortalized human diploid fibroblasts cell line (IHF). Using specific probes to chromosomes 1 and 9 (chosen based on chromosome size, probe efficiency, and reported instability found in tumors), several types of aberrations were observed including polyploidy, aneuploidy, chromosomal breaks, and telomere translocations. The most prevalent aberration was polyploidy. Abnormally large cells and nuclei, indicative of polyploidy, were also observed at high frequency in populations of interphase cells (data not shown). An example of polyploidy revealed by chromosome painting is shown in Figure 1d, where a diploid control cell is compared to a tetraploid cell resulting from cyclin E deregulation. Chromosomes from mitotic spreads of cyclin E deregulated cells also appeared hypercondensed compared to those in control spreads (see Discussion).

Flow cytometry was used to screen for cell cycle abnormalities resulting from cyclin E deregulation. Previous studies have shown that cells deregulated for cyclin E expression accumulate in S phase (Ekholm-Reed et al., 2004a; Ohtsubo and Roberts, 1993; Resnitzky et al., 1994). FACS profiles of asynchronous cyclin E and control retrovirus-transduced asynchronous cells labeled with propidium iodide (PI) confirmed this observation but also revealed an increase in G2/M cells (retro Cyclin E = 21%; retro control = 10%) (Figure 1e). For better resolution of S phase and G2/M populations, replicating (S phase) DNA was labeled with a 20-minute bromodioxyuridine (BrdU) pulse. Figure 1f shows a representative FACS profile of IME cells transduced with cyclin E and control adenovirus in order to observe acute effects on the cell cycle. Deregulation of cyclin E led to an accumulation of S phase (ad cyclin E = 13.4%, ad Cont = 9.6%) and G2/M (ad cyclin E = 17.3%, ad Cont = 12%) cells.

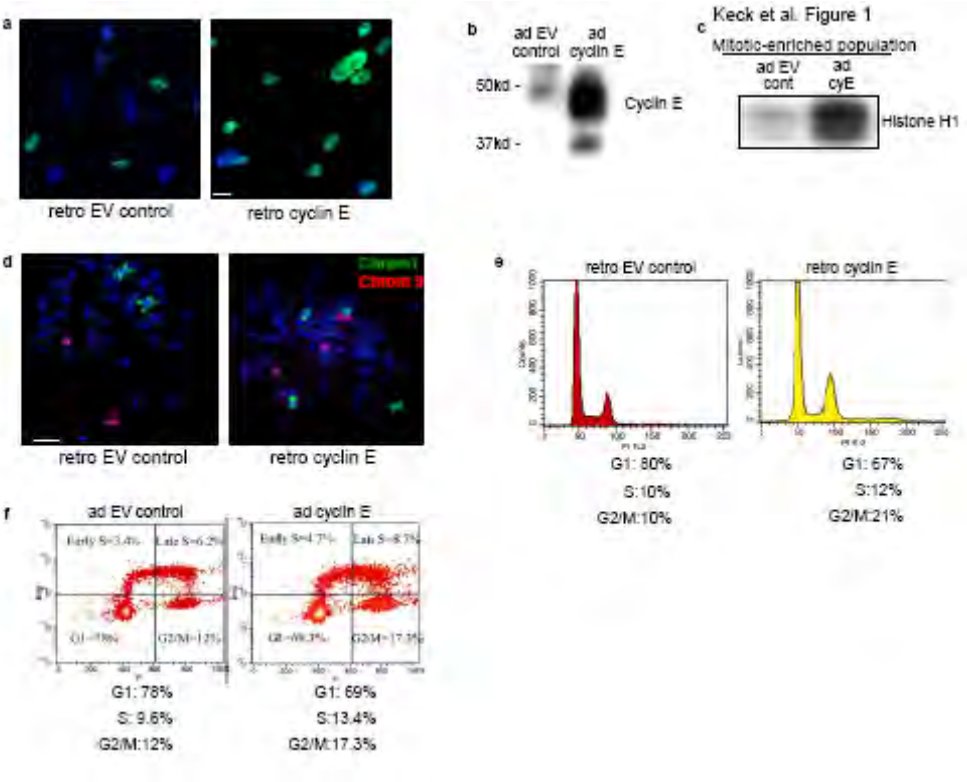

Figure 1: Deregulated cyclin E expression and kinase activity leads to an accumulation of S and G2/M populations and polyploidy. a.) Immunofluorescence microscopy showing immortalized mammary epithelial (IME) cells following transduction with a retrovirus expressing a hyperstable cyclin E mutant (T380A) or with empty-vector (EV) control. Cyclin E antibody, green; DAPI counterstaining of DNA, blue. Size bar = 10μm. **b.)** Western blot comparing expression of cyclin E in KB cells 24 hours after transduction with an adenovirus expressing wild-type cyclin E (ad cyclin E) or with empty vector (EV-control). **c.)** Histone H1 kinase assay of cyclin E-Cdk2 from M-phase enriched cells. KB cells were transduced with cyclin E or EV-control adenovirus and then enriched for mitotic cells using a single thymidine block, followed by an eight-hour release in the presence of nocodazole. Cell lysates were immunoprecipiated with anti-Cdk2 and the immune complexes were subjected to an in vitro kinase assay using purified histone H1 as a substrate. **d.)** Analysis of ploidy in retrovirus-transduced cells by chromosome painting. Chromosome 1 (green) and chromosome 9 (red) paints were hybridized to metaphase spreads prepared from IHF cells arrested in 100nM nocodazole for 6 hours. In the control cell, a normal diploid karyotype is shown, whereas a tetraploid karyotype is shown in the cell deregulated for cyclin E expression. Size bar = 5μm. **e.)** Cell cycle analysis of retrovirally transduced cells by flow cytometry. DNA content of cells transduced with retrovirus expressing cyclin E or with empty vector control was measured by intensity of propidium iodide staining, shown on the Y-axis. The percentages of cells in G1 (2N DNA content), S phase (in between 2N and 4N), and G2/M (4N DNA content) were determined using CellQuest (Becton-Dickinson). **f.)** Cell cycle analysis of adenovirus-transduced KB cells by 2-dimensional flow cytometry. Asynchronous KB cells were transduced with cyclin E or EV-control adenovirus for 24 hours followed by a 20-minute incubation with BrdU and then stained with propidium iodide to determine the DNA content and anti-BrdU antibody to resolve the S phase

population.

Cyclin E deregulation leads to an early mitotic delay.

The flow cytometry experiments described above revealed an accumulation of cells with 4N DNA content. However, these experiments were unable to distinguish G2 from mitotic populations. Immunostaining cells with an antibody reactive with phosphorylated histone H3 (H3-P) gives a distinct punctate pattern beginning at centromeres in G2 cells and brightly covering entire chromosomes in mitotic cells (Hendzel et al., 1997). Figure 2a demonstrates the nuclear pattern associated with G2 cells. The onset of histone H3 phosphorylation in U2OS cells was confirmed to begin in late S phase to early G2 by labeling cells with both anti-H3-P and anti-BrdU antibodies after a short BrdU pulse (data not shown). Scoring interphase U2OS cells for positive H3-P staining demonstrated a decreased G2 population in cyclin E adenovirus-transduced cells (ad control = 12%, ad cyclin E = 6%) (Figure 2a). These data indicate that the G2/M accumulation, previously shown by FACS analysis in cells deregulated for cyclin E expression, is due to an accumulation of cells in mitosis rather than in G2.

To determine if cyclin E deregulation leads to accumulation of cells at a particular stage of mitosis, the distribution of mitotic phases was scored in asynchronous populations using immunofluorescence microscopy. KB cells were transduced with cyclin E or control adenovirus for 24 hours, fixed, and immunostained with anti-H3-P to highlight mitotic cells, anti-α–tubulin to label mitotic spindles, and a centromere binding protein antibody. Mitotic phases were then scored based on the positions of chromosomes and the orientation of the mitotic spindle. Six mitotic phases were classified and scored in the analysis: prophase, prometaphase, unaligned metaphase, metaphase, anaphase-telophase, and cytokinesis (Figure 2b). Prophase was scored as the interval from chromosome condensation to nuclear envelope breakdown. Prometaphase was scored as the interval characterized by congression of chromosomes toward the metaphase plate and the establishment of a bipolar mitotic spindle. Unaligned metaphase was scored in cases where cells had an established bipolar mitotic spindle

and bioriented chromosomes, but exhibited incomplete alignment of chromosomes and centromeres on the metaphase plate. Metaphase was scored as the interval from complete alignment of chromosomes and centromeres on the metaphase plate until separation of sister chromatids. Anaphase-telophase was scored during poleward movement of chromosomes until the loss of H3-P labeling and the beginning of chromosome decondensation. Finally, cytokinesis was scored in cells containing decondensed chromosomes and connected by an intercellular bridge and midbody.

Results from such mitotic counts indicate deregulation of cyclin E expression leads to accumulation of KB cells in prometaphase (ad cyclin E = 31%, ad control = 24% of mitotic cells counted) and unaligned metaphase (ad cyclin E = 20%, ad control = 13%) compared to control cells (Figure 2c). The accumulation of cells at early stages of mitosis appears to include later stages of prometaphase up until the interval of alignment of chromosomes on the metaphase plate, but not including the point of complete chromosome alignment. Consequently, the aligned metaphase population was decreased as a percentage of the entire mitotic population (ad cyclin E = 13%, ad control = 19%). However, once cells deregulated for cyclin E expression recover from the delay and proceed into anaphase, they traverse the later phases of mitosis without delay relative to controls.

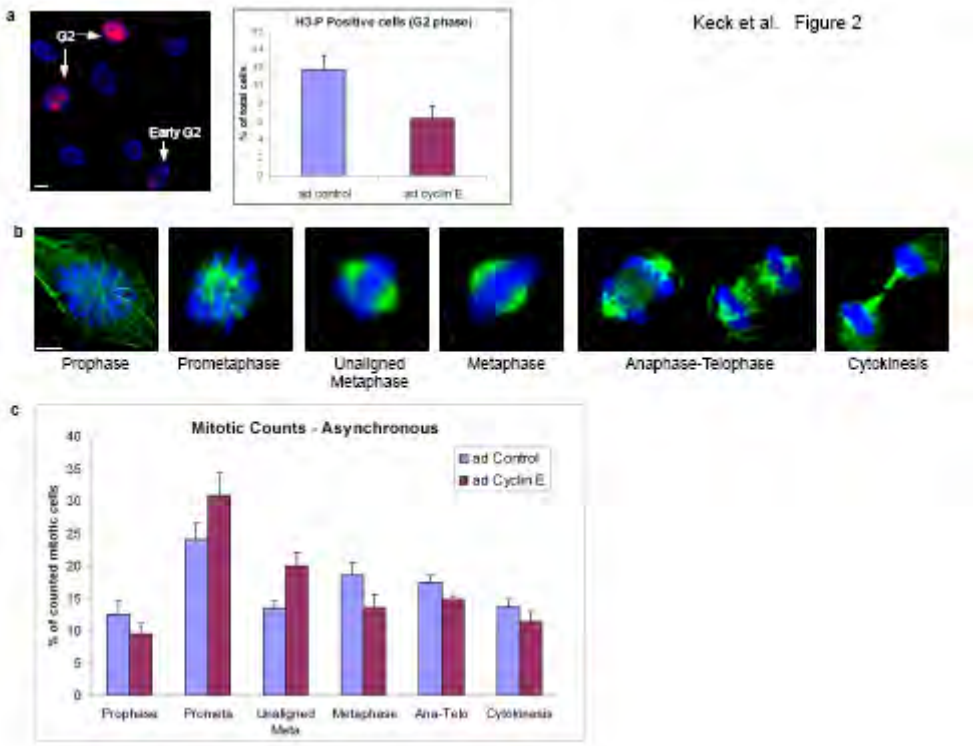

Figure 2. **Cells deregulated for cyclin E accumulate in early mitosis rather than G2. a.)** A representative immunofluorescence image of U2OS cells, acquired using deconvolution microscopy, showing phosphorylated histone H3 (H3-P) in red and DNA based on DAPI staining in blue. A graph showing the percentage of H3-P-positive interphase cells in an asynchronous population when transduced with either cyclin E or EV-control retrovirus. Error bars represent standard error based on four experiments counting 600 cells. Size bar = 10μm. **b.)** Examples of cells in the six mitotic phases scored in this study for fixed-cell mitotic counts in an asynchronous population: Prophase, Prometaphase, Unaligned metaphase, Metaphase, Anaphase-Telophase, and Cytokinesis. DNA was detected using DAPI (blue) and microtubules were detected using anti-tubulin antibodies (green). Size bar = 5μm. **c.)** Graph comparing the percentages of cells in each mitotic phase out of the total of mitotic cells counted, following transduction with EV-control or cyclin E adenovirus. n=300 mitotic cells counted in five experiments. Error bars represent standard error.

An early mitotic delay is observed by live-cell microscopy.

For a more complete analysis of mitotic defects caused by deregulation of cyclin E, mitotic division was observed in real-time. For these experiments, a recombinant retrovirus was engineered to ectopically express histone H2B tagged with GFP (H2B-GFP). IME and U2OS cells were transduced with the H2B-GFP retrovirus and selected for stable expression in order to observe dynamics of mitotic

chromosomes. Cells transduced with cyclin E or control adenovirus were filmed as they progressed through mitosis using a deconvolution microscope equipped with a closed-chamber system to maintain pH and temperature. Five Z-sections with a 3-μm step were acquired once per minute using both DIC and fluorescence optics.

The recordings of IME and U2OS cells provided direct real-time evidence that deregulated expression of cyclin E confers an early mitotic delay. In addition, they provided insight into the dynamics of the prometaphase delay. For live-cell recordings, unaligned metaphase could not be accurately determined due to the lack of spindle and centromere labels. Therefore, prometaphase was scored as the time from chromosome congression toward the midzone until all chromosomes were completely aligned at the metaphase plate. Figure 3d shows the average time, in minutes, of prometaphase, metaphase, and anaphase-telophase based on recordings of control or cyclin E adenovirus-transduced cells undergoing mitosis. Cyclin E deregulated cells spent, on average, almost two-fold longer in prometaphase than controls (ad cyclin E = 26-29 mins, ad control = 11-16 mins, depending on cell type). In some abnormal mitoses characteristic of cyclin E-deregulated cells, chromosomes oscillated near to the metaphase plate for an extended period before finally progressing into anaphase, with either aligned or unaligned chromosomes. Figure 3a illustrates mitotic division in a control U2OS cell. Prometaphase is approximately 15 minutes and metaphase begins at 20 minutes (indicated by the red asterisks). Figures 3b and 3c show mitotic divisions in cells deregulated for cyclin E expression with delayed and abnormal prometaphases. In the second series of a cyclin E-transduced IME cell (Figure 3b) shows an abnormal prometaphase (longer than 30 mins), during which chromosomes never progressed to a successful metaphase and began anaphase after 38 minutes, despite a failure of chromosome alignment. In the third series of a cyclin E-transduced U2OS cell (Figure 3c, also shown in supplementary movie 1), a prometaphase delay was observed for almost 40 minutes, during which chromosomes nearly aligned at the metaphase plate but proceeded to oscillate near the plate for a prolonged period until the recording

ended. Another demonstration of a cell deregulated for cyclin E expression that delays prior to complete metaphase alignment is shown in supplementary movie 2.

In addition to the early mitotic delays, mitotic failures were observed in which cells deregulated for cyclin E expression did not progress into anaphase but instead began to decondense chromosomes, resulting in a polyploid cell (supplementary movie 3). This was consistent with our observation of an accumulation of polyploid cells in cyclin E-deregulated populations. Together, analysis of mitosis in both fixed and live cells suggests that a primary consequence of cyclin E deregulation is mitotic impairment, which in extreme cases can lead to mitotic failure and polyploidy.

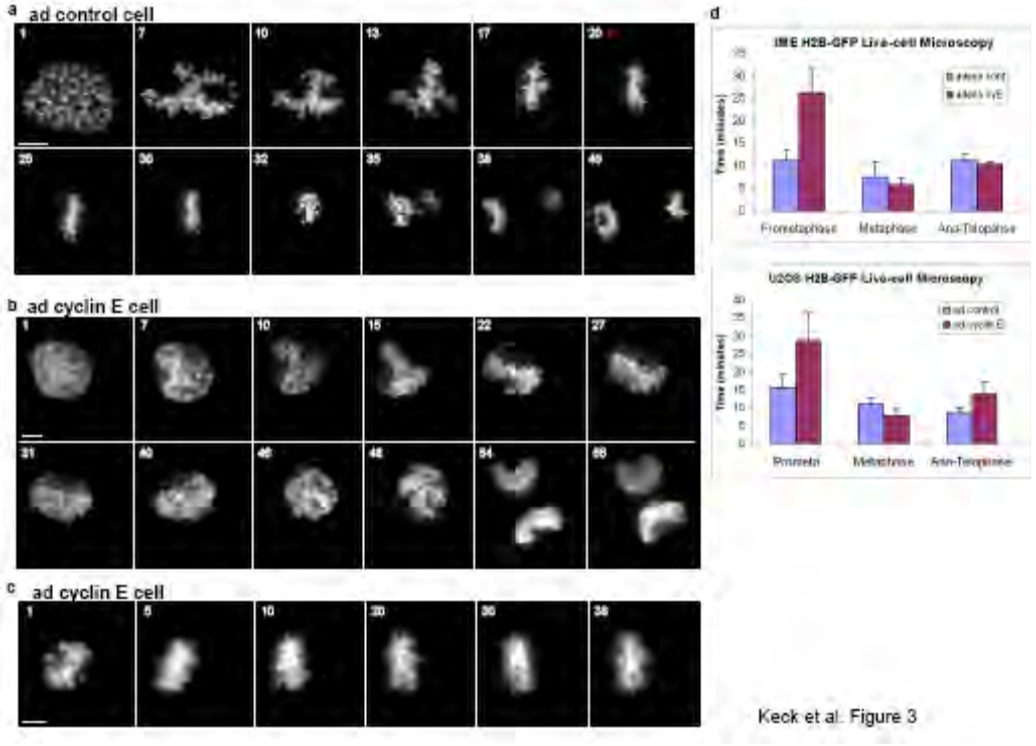

Figure 3. Quantitation of cyclin E-mediated mitotic delay by live-cell microscopy. Live-cell microscopy was performed using IME and U2OS cells expressing histone H2B-GFP for visualization of chromosome dynamics. DIC (not shown) and fluorescence (GFP) images were recorded once per minute during mitosis using a deconvolution microscope. The time elapsed after recording was initiated is indicated at the top left of each frame. Select frames are shown from representative U2OS and IME movies. Red asterisk (*) marks metaphase. **a.)** A control U2OS cell that begins in prophase, progresses into prometaphase, aligns all chromosomes by 20 mins (the longest prometaphase recorded in control cells), and initiates chromosome segregation after 31 mins. **b.)** An IME cell deregulated for cyclin E expression that begins in prophase, quickly progresses into prometaphase but never completely aligns all chromosomes. After 38 mins chromosome segregation begins despite a failed metaphase. **c.)**

A U2OS cell deregulated for cyclin E expression that begins in prometaphase and continues for 40 minutes, during which chromosomes migrate towards the metaphase plate but never completely align (also shown in supplementary movie 2). **d.)** Graphs showing the average time (minutes) that IME and U2OS cells spend in each phase of mitosis, error bars represent one standard devivation. n=5 recordings each of IME cells deregulated for cyclin E expression or controls, and 7 recordings each of U20S cells deregulated for cyclin E expression or controls. Size bars = 5μm for all images.

Cyclin B1 expression is upregulated and degradation is delayed in metaphase due to cyclin E deregulation.

In order to investigate the cause of the cyclin E-mediated mitotic delay, levels of mitotic regulatory proteins were determined. Single cell analysis of cyclin B1 expression was used to compare peak levels of cyclin B1 in early mitosis and its degradation in metaphase in cells deregulated for cyclin E expression and controls. KB cells were released for eight hours into mitosis from a single thymidine block. Representative images of mitosis in cells transduced with either control or cyclin E adenovirus are shown in Figure 4a. Cyclin B1 (green), a centromere-binding protein (red) and DNA (blue) were labeled and cyclin B1 levels were measured in early prometaphase cells, unaligned metaphase cells, and metaphase cells. Using ImageJ analysis software (Rasband, 2005), cyclin B1 staining intensities of each cell, were divided into “low”, “medium”, and “high” categories (Figure 4b). As can be seen, deregulation of cyclin E led to elevated levels of cyclin B1 in prometaphase and unaligned metaphase. Furthermore, in metaphase, all control cells expressed low levels of cyclin B1, as expected due to its degradation by the mitotic ubiquitin ligase APC^{Cdc20}. However, the degradation of cyclin B1 was delayed in 45% of metaphase cells with cyclin E deregulation, which continued to express medium and high levels of cyclin B1 (Figure 4b, Metaphase). These results suggest that deregulation of cyclin E can delay normal degradation of cyclin B1. However, cyclin B1 degradation was not completely inhibited, as anaphase cells from both control and cyclin E deregulated cells contained low levels of cyclin B1 (data not shown).

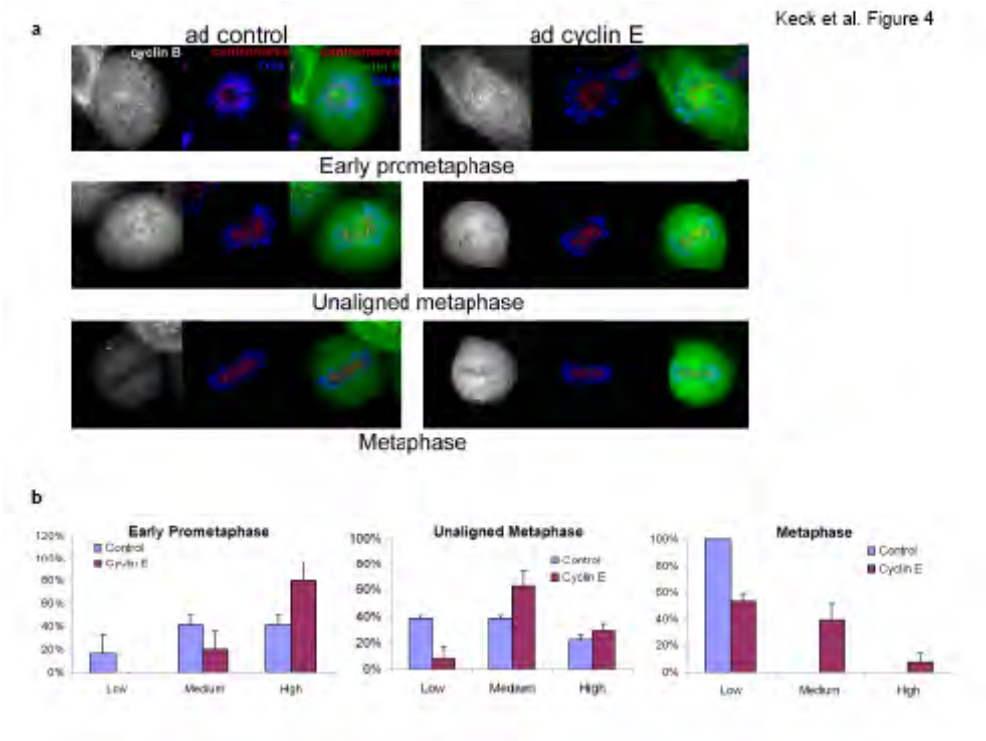

Figure 4. Cyclin E deregulation leads to excessive accumulation of cyclin B1 during prometaphase and a delay in cyclin B1 degradation during metaphase. **a)** Immunofluorescence images comparing KB cells transduced with either EV-control adenovirus (left column) or cyclin E adenovirus (right column) in early prometaphase, unaligned metaphase, and metaphase. Cyclin B1, a centromere-binding protein, and DNA were stained in fixed cells, and images were acquired using a deconvolution microscope **b.)** Graphs from early prometaphase, unaligned metaphase or metaphase populations showing the percentage of EV-control and cells deregulated for cyclin E with low, medium, or high cyclin B1 levels. ImageJ was used to measure average pixel intensities of cyclin B1 in cells from 8-bit grayscale images. The area of each cell was used to account for variations in cell size. Cyclin B levels were arbitrarily divided into low, medium, and high groupings. The X-axis, cyclin B1 level; Y-axis, the percentage of the total number of cells. n=10 control and cyclin E deregulated cells, each, per mitotic phase. Error bars correspond to the variance based on two experiments.

Cyclin E deregulation causes accumulation of APC substrates up to and through mitosis.

Next, protein levels of other important APC/C substrates were assessed during mitosis. For these experiments, cells were transduced with adenovirus and simultaneously arrested in a single thymidine block overnight. As adenoviral cyclin E is not expressed significantly prior to eight hours following transduction (data not shown), the majority of non-thymidine blocked cells will have passed through mitosis and early G1 prior to cyclin E accumulation. Therefore, this protocol precludes S phase defects

conferred by cyclin E-mediated interference with pre-replication complex assembly in late telophase. In addition, the single thymidine block and release protocol ensures approximately equal percentages of cells in G2/M for each time point collected, as monitored by FACS anaylsis (Figure 5a). In KB cells, the peak of mitosis based on microscopic observation occurs from 8 to 10 hours following release from a thymidine block. Western blot analysis of protein expression up to and through mitosis in cyclin E deregulated and control cells revealed an accumulation of cyclin B1, Cdc20, and securin (Figure 5b). Quantification and normalization of these data are shown in Figure 5c. In cells deregulated for cyclin E expression, mitotic protein levels were elevated relative to controls at each time point up to and through the peak mitotic samples. These data indicate that defects in mitotic protein expression are not cyclin B-specific, but suggest rather that the APC/C ubiquitin ligase is inhibited under conditions of cyclin E deregulation, as all of the proteins exhibiting elevated expression are APC/C substrates targeted for ubiquitin-mediated proteolysis.

Cyclin E-induced accumulation of mitotic regulatory proteins is due to increased stability.
In order to determine whether the observed protein accumulations were due to decreased degradation, we examined protein stability by carrying out cyclohexamide chase experiments under conditions of cyclin E deregulation. Cells transduced with cyclin E or control adenovirus and arrested using a single thymidine block were then released for four hours. Cyclohexamide was added to terminate protein synthesis and samples were collected, as indicated, for Western blot analysis (Figure 5d). Quantification and normalization of these data are shown in Figure 5e. As can be seen, cyclin B1, securin, and Cdc20 were degraded much more rapidly in control cells compared to cells deregulated for cyclin E expression, suggesting that cyclin E-mediated accumulation of key mitotic regulatory proteins occurs by decreasing their rate of ubiquitin-mediated proteolysis.

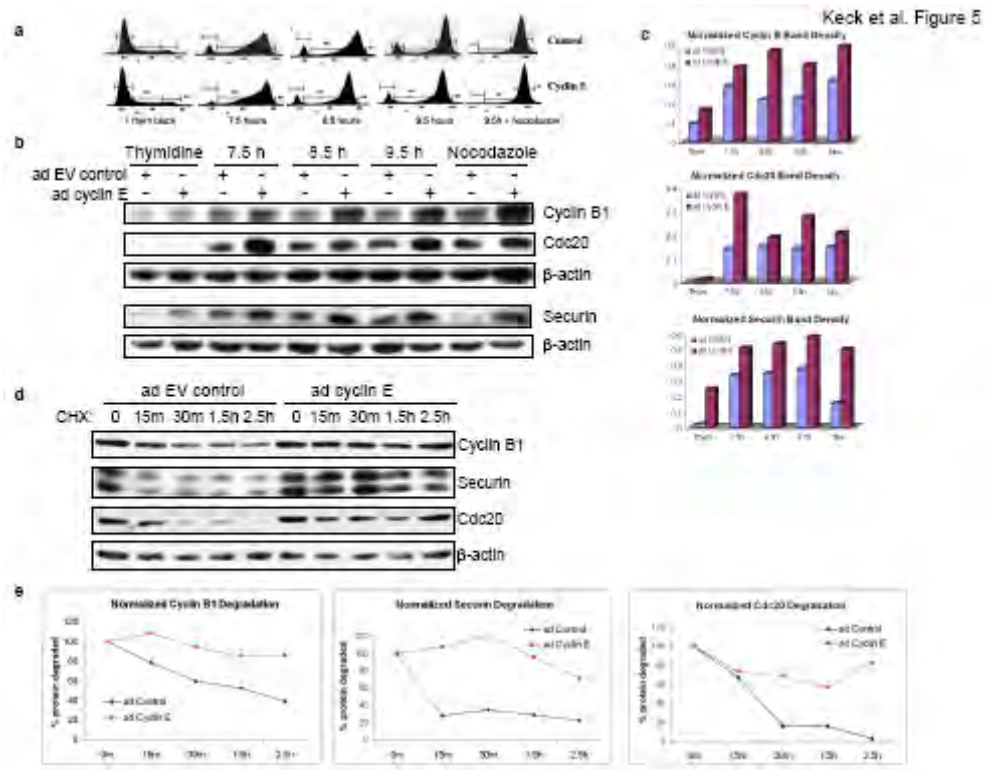

Figure 5. Cyclin E deregulation causes the accumulation of APC/C substrates up to and through mitosis due to increased protein stability. a.) Representative FACS profiles (PI staining) from EV-control and cyclin E adenovirus transduced KB cells collected at specific times after release from a thymidine block. **b.)** Representative Western blot analyses showing elevated expression of APC/C substrates cyclin B, Cdc20, and securin in cyclin E deregulated cells compared to control cells. β-actin is used as a loading control in both experiments. **c.)** Band densities from (b) quantified and normalized to actin. **d**.) Western blot analysis of a cyclohexamide-chase experiment showing stabilization of APC/C substrates under conditions of cyclin E deregulation. Degradation of cyclin B, securin, and Cdc20 was assayed following thymidine synchronization and a 4-hour release into late S/G2 phase. Cyclohexamide was added at 0 mins and samples were collected at 0 mins, 15 mins, 30 mins, 1.5 hrs, and 2.5 hrs, following cyclohexamide addition. **e**.) Quantitation of cyclohexamide-chase experiment in (d). Band intensities were normalized to actin.

Overexpressed cyclin E-Cdk2 binds and phosphorylates Cdh1.

The data presented up to this point suggest that deregulated cyclin E-Cdk2 inhibits the APC/C, leading to increased expression of important mitotic regulatory proteins thus causing mitotic delay prior to metaphase. APC/C activity requires one of two activating regulatory subunits, Cdc20 or Cdh1 (Kramer et al., 2000; Visintin et al., 1997). Cdc20 is thought to activate the APC/C during mitosis whereas Cdh1 is the activating subunit from mitotic exit to the G1-S boundary (Blanco et al., 2000; Fang et al., 1998;

Jaspersen et al., 1999; Kramer et al., 2000; Lukas et al., 1999; Sorensen et al., 2000). Since Cdc20 itself was found to accumulate in response to cyclin E deregulation, it was unlikely to be the relevant target of cyclin E-Cdk2. On the other hand, Cdh1 is inactivated by phosphorylation and is thought to already be inactive during early mitosis due the phosphorylation by cyclin A-Cdk2 (Lukas et al., 1999; Sorensen et al., 2001). Furthermore, under normal circumstances, it was shown that cyclin E-Cdk2 does not contribute significantly to Cdh1 phosphorylation and inactivation (Brandeis and Hunt, 1996; Lukas et al., 1999; Sorensen et al., 2001).

To determine whether Cdh1 is a substrate of cyclin E-Cdk2 and therefore potentially inhibited by cyclin E deregulation, binding and phosphorylation assays were carried out. We first determined whether cyclin E-Cdk2 could bind directly to Cdh1, since protein kinases often form stable complexes with substrates. Cyclin A binding to Cdh1 has previously been described and was used as a positive control (Lukas et al., 1999; Sorensen et al., 2001). Three expression plasmids coding for N-terminally Myc-tagged wild-type (WT) or mutants, $Cdh1^{RVL\text{-}AAA}$ and $Cdh1^{4A}$, were used to characterize binding of cyclin E and cyclin A to Cdh1 (Sorensen et al., 2001). $Cdh1^{RVL\text{-}AAA}$ is mutated in the WD-40 repeat domain at the RVL motif shown to be necessary for cyclin A binding, and $Cdh1^{4A}$ is mutated at four phosphorylation sites shown to be targeted by cyclin A-Cdk2 that are essential for Cdh1 inhibition. Expression plasmids for cyclin E or cyclin A were co-transfected with expression plasmids encoding $Cdh1^{WT}$, $Cdh1^{AAA}$, $Cdh1^{4A}$, or an empty vector into 293T cells. Samples were collected 48 hours later and Cdh1 was immunoprecipitated from lysates using anti-Myc antibody. The immunoprecipitation data show that exogenous cyclin E binds efficiently to $Cdh1^{WT}$, as does the positive control, cyclin A (Figure 6a). In addition, weak binding is detectable between exogenous cyclin A and both Cdh1 mutants. Exogenous cyclin E also bound both wild-type and, to a lesser degree, both mutant Cdh1 mutants. However, no binding was observed at endogenous levels of cyclin E (shown as band with lower mobility than exogenous cyclin E), consistent with previous results (Sorensen et al., 2001), and suggesting that cyclin E interacts with Cdh1 with lower affinity than does cyclin A.

To determine whether Cdh1 is a substrate of cyclin E-Cdk2, in vitro phosphorylation assays were carried out. GST-Cdh1 (Sorensen et al., 2001) and GST alone were purified from E. coli. In vitro kinase assays were performed using cyclin E-Cdk2 and cyclin A-Cdk2 purified from baculovirus-transduced insect cells on histone H1, GST, and GST-Cdh1 as substrates (Figure 6b). Robust phosphorylation of histone H1 by cyclin E-Cdk2 and cyclin A-Cdk2 confirmed that both kinase complexes were active. GST alone (~28kD) was not phosphorylated by either cyclin-Cdk2 complex. However, purified GST-Cdh1 (75kD), as well as a number of degradation products, was phosphorylated by both cyclinE-Cdk2 and cyclin A-Cdk2.

Phosphorylation of Cdh1 was also confirmed in cell culture. In Figure 6a, reduced mobility was shown for $Cdh1^{WT}$ and $Cdh1^{RVL\text{-}AAA}$ when co-expressed with either cyclin E or cyclin A. To ensure that the reduced mobility was due to phosphorylation of Cdh1, parallel samples, using $Cdh1^{WT}$, were treated with λ–phosphatase to dephosphorylate Cdh1 prior to analysis (Figure 6c). Cdh1 exhibited reduced mobility upon co-transfection of either cyclin E or cyclin A. This mobility shift was reversed with phosphatase treatment, but not when phosphatase inhibitors were present, indicating that ectopically expressed Cdh1 can be phosphorylated by either cyclin E-Cdk2 or cyclin A-Cdk2.

Next, we assessed the ability of cyclin E-Cdk2 to phosphorylate endogenous Cdh1 under conditions where cyclin E-mediated accumulation of mitotic APC/C substrates was observed (as in Fig. 5). Samples were collected up to and through mitosis following a thymidine block and release (Fig. 6d). Deregulation of cyclin E reduced the mobility of endogenous Cdh1 (Fig. 6d), consistent with cyclin E-Cdk2 contributing significantly to the phosphorylation and inactivation of Cdh1 under these conditions.

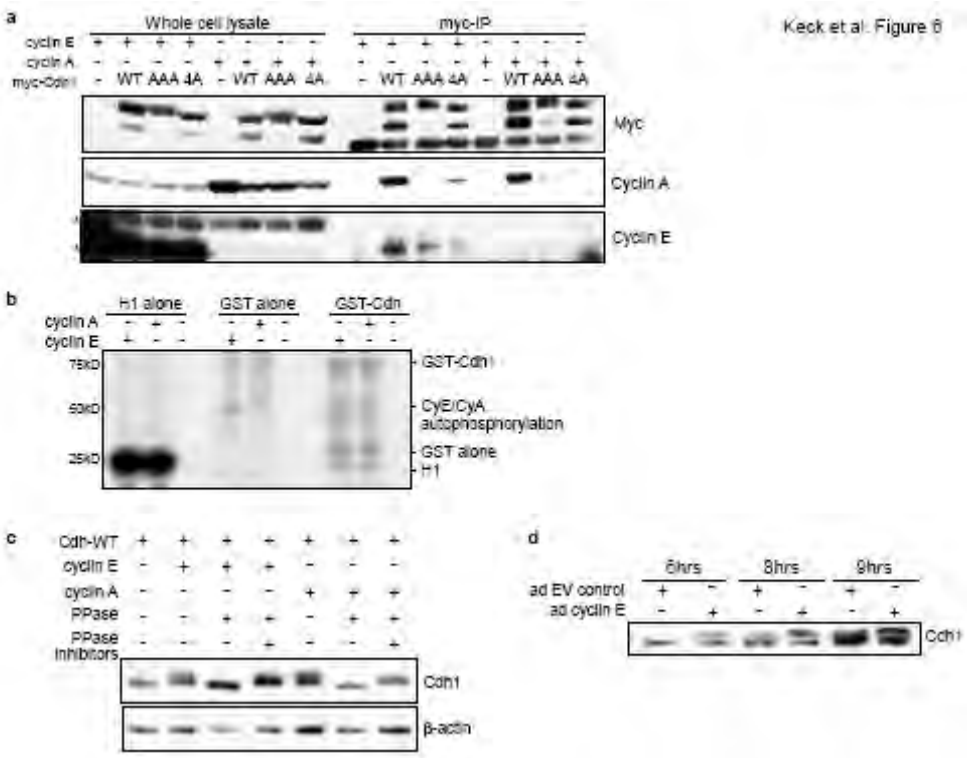

Figure 6. Cyclin E and cyclin A can bind and phosphorylate the APC-activating subunit, Cdh1. a.) Immunoprecipitation assay using empty vector or one of three Myc-tagged Cdh1 constructs: WT (wild-type), AAA (an RxL motif cyclin-binding mutant), or 4A (a phosphorylation-site mutant). Cdh1 and cyclin E or cyclin A expression plasmids were transiently transfected into 293T cells. Cell lysates were immunoprecipitated with anti-Myc antibody, separated by SDS-PAGE, and detected by Western blot. Both exogenous and endogenous cyclin A are detected using anti-cyclin A. Endogenous and exogenous cyclin E are detected using anti-cyclin E antibody (endogenous cyclin E is observed migrating more slowly than exogenous, both marked with asterisks). **b.)** In vitro kinase assay with GST-Cdh1 purified from *E. coli*. Purified cyclin E-Cdk2, cyclin A-Cdk2, or buffer were incubated with γ-^{32}P ATP and either histone H1 (first three lanes), GST (second three lanes) or GST-Cdh1 (third three lanes). **c.)** Cdh^{WT} exhibits reduced mobility upon co-tranfection of cyclin E or cyclin A due to increased phosphorylation. Transfection of 293T cells was performed as described in (a). Cell lysates were incubated with λ-phosphatase in the presence or absence of phosphastase inhibitors, as indicated. Lysates were separated by SDS-PAGE and immunoblotted using anti-Cdh1 antibody for detection. β-actin serves as a loading control. **d.)** Western blot showing phosphorylation of endogenous Cdh1 in KB cells transduced with adenoviral cyclin E. Cells were transduced with EV-control or cyclin E adenovirus, arrested using a single thymidine block, and released. Samples were collected as cells progressed into and through mitosis and analyzed for Cdh1 migration by SDS-PAGE followed by Western blot and detection using anti-Cdh1 antibody. Slower migrating band represents hyperphosphorylated Cdh1 based on experiment shown in (c).

Cyclin E-Cdk2 inhibits APC^{Cdh1} –dependent ubiquitylation of cyclin B1 in vitro

To assess the effects of cyclin E-Cdk2 on the activity of the APC^{Cdh1} directly, in vitro ubiquitylation assays were performed (Figure 7). Cdh1 was phosphorylated in vitro (confirmed by a mobility shift; data not shown) prior to addition to the ubiquitylation reaction. APC^{Cdh1} activity was determined by the conversion of unmodified cyclin B1 to a ladder of multi-ubiquitylated cyclin B1 derivatives.

Cyclin B1 was efficiently ubiquitylated when Cdh1 was added to the reaction in the absence of cyclinE-Cdk2 (Figure 7a). Upon addition of purified cyclin E-Cdk2, ubiquitylation of cyclin B1 was dramatically reduced, indicated by a reduction in conversion of cyclin B1 to multi-ubiquitylated derivatives, consistent with phosphorylation-dependent inhibition of Cdh1 (Figure 7a and quantified in Figure 7b). The addition of purvalanol, a Cdk inhibitor, partially reversed cyclin E-mediated inhibition. These data suggest that cyclin E-Cdk2 inhibits Cdh1 via phosphorylation. Furthermore, a phosphorylation-site mutant of Cdh1, where all possible Cdk sites were mutated to alanines was completely resistant to cyclin E-Cdk2-mediated inhibition (Figure 7a and quantified in Figure 7b). These data confirm that cyclin E-Cdk2 can inactivate APC^{Cdh1} through the inhibitory phosphorylation of Cdh1.

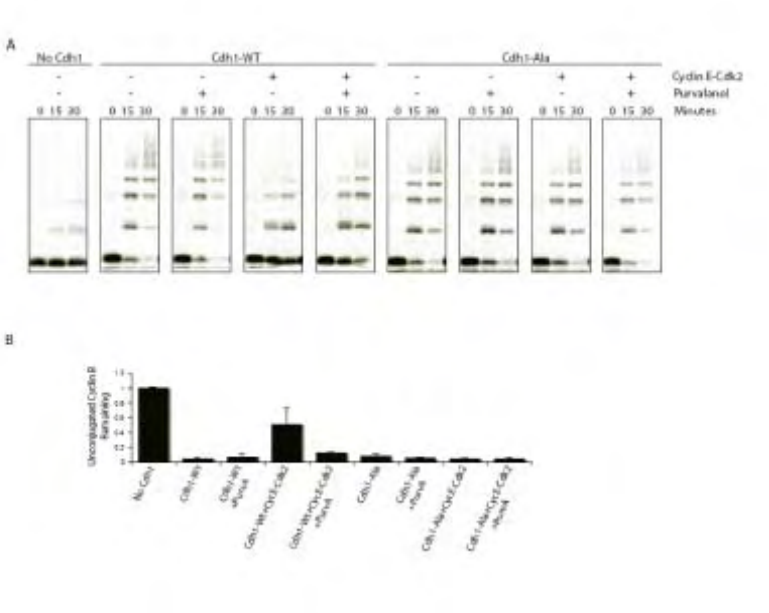

Figure 7: Cyclin E-Cdk2 inhibits APC^{Cdh1} ubiquitin ligase activity in vitro through a kinase-dependent mechanism. a.) In vitro ubiquitylation was used to assess inhibition of the APC^{Cdh1} by cyclin E-Cdk2. Cyclin B1 antibody was used to visualize both unmodified and polyubiquitylated substrate. Addition of cyclin E-Cdk2 and/or the Cdk inhibitor purvalanol to the various reactions is indicated. Reactions were carried out in parallel with wild type Cdh1 (Cdh1-WT) and a Cdk phosphorylation site mutant (Cdh1-Ala). **b.)** Quantitation of unmodified cyclin B1 in reactions shown in (a). Error bars represent the variance of the mean from two independent experiments.

Reduction of Cdh1 levels results in mitotic protein accumulation and mitotic delay similar to deregulation of cyclin E.

We have shown that cyclin E-Cdk2-mediated phosphorylation of Cdh1 is able to inhibit ubiquitylation activity of the APC^{Cdh1} in vitro. If cyclin E-Cdk2 also inhibits APC^{Cdh1} in vivo, reducing cellular levels of Cdh1 should mimic the phenotype associated with deregulation of cyclin E. Using Cdh1-specific siRNA, the effects of Cdh1 reduction were compared with those associated with cyclin E deregulation. A strong knockdown of Cdh1 protein (using 20 nM of Cdh1-specific siRNA) inhibited cell proliferation, which had previously been reported (Gimenez-Abian et al., 2005b; Sorensen et al., 2001). To only partially ablate Cdh1, the time of incubation and the concentration of Cdh1-specific siRNA were reduced. The accumulation of cyclin B1, securin, and Cdc20 in cells targeted by Cdh1-specific siRNA was compared to that in cells transduced with cyclin E or EV-control adenovirus (Figure 8a). A

comparable upregulation of cyclin B1, securin, and Cdc20 protein occurs due to both Cdh1 reduction and cyclin E deregulation.

We next determined the effects of reducing Cdh1 on mitotic progression. Fixed cells were scored, as previously discussed, in asynchronous populations following transduction of EV-control or cyclin E adenovirus for 24 hours and incubation with Cdh1-specific or GFP-specific siRNA for an additional 24 hours (Figure 8b). As shown previously, cyclin E deregulation caused an accumulation in early mitosis prior to metaphase. This same trend, with a more pronounced accumulation, was observed in cells transfected with Cdh1-specific siRNA (Figure 8b). These data confirm that Cdh1 has a role in regulation of progression through early mitosis and that cyclin E-mediated inhibition of Cdh1 could, in principle, account for impairment of early mitotic events.

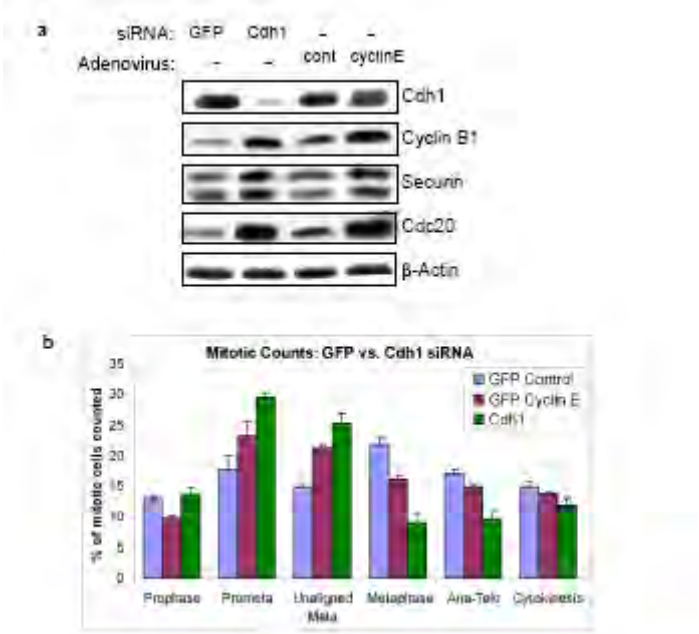

Figure 8: Reducing Cdh1 by RNAi mimics cyclin E deregulation, resulting in mitotic protein accumulation and early mitotic delay. a.) Western blot comparing the accumulation of cyclin B1, securin, and Cdc20 in cells subjected to partial silencing of Cdh1 using siRNA or deregulated for cyclin E expression. Asynchronous populations were collected and analyzed by immunoblotting. **b.)** Mitotic counts of cells subjected to Cdh1-specific RNAi. Cells were transfected with Cdh1-specific siRNA or transduced with EV-control or cyclin E adenovirus followed by transfection with GFP-specific siRNA. Mitotic phases were scored as described previously. n=300 cells per sample. Error bars correspond to standard error based on three experiments.

Reducing the levels of APC^{Cdh1} substrates cyclin B1 and securin in cells deregulated for cyclin E allows progression through mitosis without delay.

Based on the data reported above, direct reduction of Cdh1 or deregulation of cyclin E, leads to accumulation of mitotic APC/C substrates and delay in progression through early mitosis. However, whether the mitotic delay is caused by accumulation of APC/C substrates and, if so, which APC/C substrate(s) contribute to the mitotic delay remained to be determined. Based on our observations, it appeared that most chromosomes become bioriented but delay in aligning at the metaphase plate and progressing into anaphase. This phenotype is consistent with a defect in sister chromatid separation possibly caused by elevated levels of cyclin B1 and securin as cells progress into and through mitosis. Degradation of securin and cyclin B1is needed to activate separase and thereby promote cleavage of cohesin (Gorr et al., 2005; Ji et al., 2005), which is required for the separation of the sister chromatids at anaphase allowing the poleward migration of chromosomes (Gimenez-Abian et al., 2005a; Hauf et al., 2001; Uhlmann et al., 1999; Uhlmann et al., 2000). We therefore tested whether slightly reducing securin and cyclin B1 expression in cells deregulated for cyclin E expression could override the cyclin E-induced delay of early mitosis.

Cells were transduced with EV-control or cyclin E adenovirus for 24 hours and then transfected with low concentrations of siRNA (10 pM) targeting securin and cyclin B1 or GFP for an additional 24 hours. Expression of cyclin B1 and securin in asynchronous cells was compared by Western blot analysis (Figure 9a). Transfection of cells transduced with cyclin E adenovirus with cyclin B1- and securin-specific siRNA resulted in levels of cyclin B1 and securin comparable to those found in control cells, whereas cells transfected with control GFP-specific siRNA continued to exhibit elevated levels of cyclin B1 and securin. As expected, Cdc20 levels were not affected by siRNA targeting cyclin B1 and securin.

For confirmation that cyclin B1 and securin protein levels were specifically reduced in mitotic cells, protein expression was assessed, as described above, under conditions of a thymidine block and release into mitosis (Figure 9b). Cyclin B1- and securin-specific siRNAs effectively reduced securin and

cyclin B1 expression in cells deregulated for cyclin E to levels found in control cells (transduced with control adenovirus and treated with GFP-specific siRNA). In addition, immunofluorescence analysis of siRNA-treated cells showed no major mitotic defects due to these decreases in cyclin B1 or securin. Again, Cdc20 levels were not affected by the siRNA treatments.

Mitotic progression was assessed in cells with reduced levels of securin and cyclin B1, securin alone, or cyclin B1 alone mediated by siRNA transfection (Figure 9c). Reducing both cyclin B1 and securin (first graph) eliminated the delays in prometaphase and unaligned metaphase mediated by cyclin E deregulation. Metaphase, anaphase-telophase, and cytokinesis were comparable to control cells. However, reducing securin or cyclin B1 alone (second and third graphs) did not eliminate the prometaphase or unaligned metaphase delay associated with cyclin E deregulation. Therefore, depletion of securin or cyclin B1 alone is not sufficient to alleviate the mitotic inhibitory effects of cyclin E deregulation and suggests that stabilization of both proteins contributes to cyclin E-mediated mitotic delay.

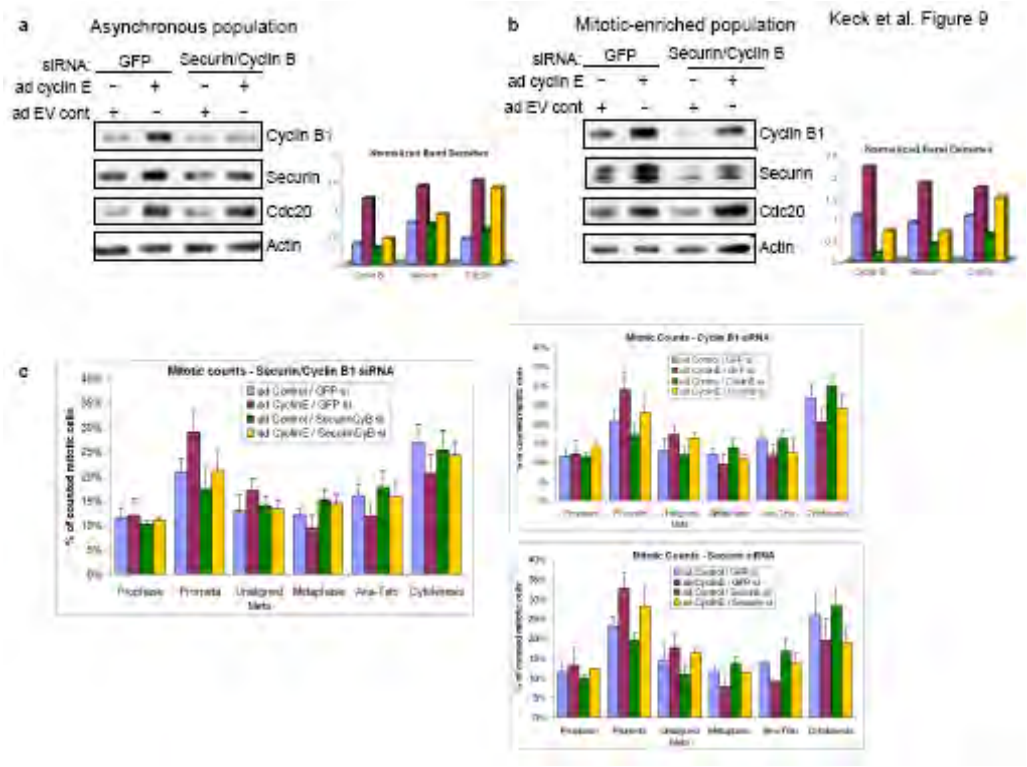

Figure 9: Reducing the accumulation of APC^{Cdh1} substrates cyclin B1 and securin in cells deregulated for cyclin E expression restores normal progression through mitosis. **a.)** Elevation of mitotic regulatory proteins cyclin B1 and securin in asynchronous cells deregulated for cyclin E expression can be reversed using low concentrations of sequence-specific siRNA. Band densities normalized to actin are shown below the Western blot. Cdc20 levels are not affected, as expected. **b.)** Elevation of mitotic regulatory proteins cyclin B1 and securin in mitotically enriched KB cells deregulated for cyclin E expression can be reversed using low concentrations of sequence-specific siRNA. Cells were treated as in (a) but subjected to a single thymidine block and harvested 8 hours after release. Band densities normalized to actin are shown below the Western blot. **c.)** Mitotic progression in cells deregulated for cyclin E expression is no longer delayed if hyperaccumulation of both cyclin B1 and securin are prevented by sequence specific RNAi. Results from mitotic counts of fixed KB cells are shown as percentages of mitotic cells in the various mitotic phases. Cells were transduced with cyclin E or EV-control adenovirus, followed by transfection with sequence-specific siRNA, as indicated, and processed for immunofluorescence, as described previously. Mitotic counts are shown for simultaneous targeting of cyclin B1 and securin (left), as well for individual targeting of cyclin B1 (top) and securin (bottom), respectively. Error bars represent standard error based on three experiments.

Discussion

Deregulation of cyclin E has been observed in a broad spectrum of human malignancies, where it

often correlates with poor prognosis (Erlandsson et al., 2003; Erlanson and Landberg, 2001; Keyomarsi et al., 1995; Nielsen et al., 1998; Spruck et al., 2002). In addition, a direct causal link between cyclin E deregulation and tumorigenesis has been established using a transgenic mouse model (Bortner and Rosenberg, 1997; Smith et al., 2006). Nevertheless, the mechanism underlying cyclin E-induced tumorigenesis has remained elusive. As cyclin E is a positive regulator of the cell-cycle kinase, Cdk2, it has been proposed that the role of cyclin E in tumorigenesis is to promote proliferation (Geng et al., 2003). On the other hand, deregulation of cyclin E was shown to cause genomic instability in cell culture models, where chromosome losses and gains as well polyploidy were observed (Spruck et al., 1999). The oncogenic properties of cyclin E may then simply reflect that genomic instability creates an unstable genetic environment that is conducive for malignant progression.

In terms of the mechanism whereby cyclin E deregulation might undermine genomic instability, we have reported that expression of cyclin E during mitotic exit impairs pre-replication complex assembly and the subsequent S phase, possibly promoting chromosome instability (Ekholm-Reed et al., 2004a). We report here, however, that deregulation of cyclin E impacts directly and adversely on mitosis. Specifically, inappropriate cyclin E activity during S phase, G2 and early M phase inhibits residual APC^{Cdh1} ubiquitin ligase activity leading to abnormal accumulation of mitotic regulatory proteins. The ultimate consequences are delay and/or failure in the early phases of mitosis leading to tetratraploidy as well as mitotic aberrations such as progression into anaphase without complete chromosome alignment. It is therefore likely that these effects of cyclin E deregulation contribute directly to genomic instability.

Inhibition of APC^{Cdh1} affects progression through early stages of mitosis.

Although Cdh1 can activate both mitotic and interphase APC/C, models of cell cycle regulation have proposed that the ubiquitin ligase ACP^{Cdh1} is maintained in an inactive state from the G1-S boundary until mitotic exit due phosphorylation by cyclin-dependent kinases active during this interval (Blanco et al., 2000; Jaspersen et al., 1999; Kramer et al., 2000; Lukas et al., 1999; Sorensen et al., 2001; Zachariae

et al., 1998). While there is evidence that cyclin E-Cdk2 is primarily responsible for accumulation of G2/M cyclins and Cdh1 phosphorylation in *Drosophila* (Knoblich et al., 1994; Sigrist and Lehner, 1997), in mammalian cells it was shown that cyclin A-Cdk2 specifically phosphorylates Cdh1 on a number sites and that this phosphorylation prevents association with the APC/C core (Lukas et al., 1999; Sigrist and Lehner, 1997; Sorensen et al., 2001). Since cyclin A-Cdk2 becomes active at the G1-S transition, and persists until early mitosis, it has been assumed that Cdh1 does not contribute to APC/C ubiquitin ligase activity during this interval and that only an alternative APC/C cofactor, Cdc20, carries out mitotic functions. However, in the current study, we show that residual APC^{Cdh1} activity must contribute to regulation of mitotic proteins up to and through early mitosis. Specifically, partially silencing of Cdh1 by RNAi led to a hyperaccumulation of APC substrates and impaired progression through early phases of mitosis. Therefore, APC^{Cdh1} must retain residual activity prior to mitosis even in the presence of cyclin A-Cdk2. This conclusion along with the observed ability of cyclin E-Cdk2 to phosphorylate Cdh1 in vivo and inhibit APC^{Cdh1} in vitro is consistent with a model where cyclin E-mediated effects on mitosis are due to inhibition of residual APC^{Cdh1} activity.

This proposal is seemingly at odds with previous reports that cyclin E-Cdk2 does not bind to Cdh1 or contribute to its phosphorylation in mammalian cells (Lukas et al., 1999; Sorensen et al., 2001). Indeed, we could not detect association between endogenous cyclin E and Cdh1. However, when expression of cyclin E was deregulated by transfection, association of cyclin E with Cdh1 and cyclin E-mediated hyperphosphorylation of Cdh1 were readily detectable. These data suggest that cyclin E, when normally expressed at the G1-S boundary, is unlikely to have a major impact on Cdh1 regulation. However, deregulated cyclin E, either in the experimental contexts reported here, or in the course of tumorigenesis, can influence Cdh1 activity in a functionally significant manner. Whether temporal deregulation of cyclin E expression or simply deregulation of cyclin E levels, or both, allow cyclin E to have an impact on Cdh1 activity remains to be determined.

APC^{Cdh1} targets relevant to cyclin E-mediated impairment of mitosis.

Deregulation of cyclin E causes cells to delay in mitosis prior to anaphase. This phenotype could be explained by a cyclin E-mediated failure to activate the mitotic protease separase. Indeed, it has been reported that one defect caused by RNAi-mediated depletion of separase is a prometaphase delay similar to that reported here in the context of cylin E deregulation (Gimenez-Abian et al., 2005a). In addition, depletion of separase induces polyploidy (Waizenegger et al., 2002). Separase specifically cleaves the cohesin subunit Scc1 resulting in loss of centromeric sister chromatid cohesion in mammalian cells, potentiating anaphase (Hauf et al., 2001; Uhlmann et al., 1999; Uhlmann et al., 2000; Waizenegger et al., 2000). The primary mode of separase regulation is through the binding of the separase inhibitor, securin (Cohen-Fix et al., 1996; Zou et al., 1999). Securin ubiquitylation by the APC/C targeting it for proteasomal degradation during the early phases of mitosis is thought to constitute the principal mitotic regulatory role of the APC/C. However, the role of securin ubiquitylation during early mitosis has been attributed to the APC/C cofactor Cdc20 rather than Cdh1, as the latter cofactor has been assumed to be inactive during this interval (see above) (Jaspersen et al., 1999; Salah and Nasmyth, 2000; Visintin et al., 1997; Zachariae et al., 1998). Indeed in yeast, inactivation of Cdc20 leads to metaphase arrest whereas inactivation of Cdh1 has no obvious effects on early stages of mitosis (Cohen-Fix et al., 1996; Kramer et al., 2000; Sigrist et al., 1995). Nevertheless, we show that in mammalian cells partial silencing of Cdh1 by RNAi leads to accumulation of securin and an early mitotic delay and it has been reported that mammalian APC^{Cdh1} shares the capacity to target securin with APC^{Cdc20} (Zur and Brandeis, 2001). Therefore it was reasonable to consider securin the relevant anaphase inhibitory target stabilized by cyclin E-mediated inhibition of Cdh1. However, when securin expression was adjusted by partial RNAi-mediated silencing so that cyclin E deregulation restored securin to normal levels, early mitotic delay was not abrogated. Recent reports have suggested that cyclin B1-Cdk1 also inhibits separase, raising the possibility that abnormal accumulation of cyclin B1 during early mitosis may also contribute to cyclin E-mediated mitotic delay (Gorr et al., 2005; Ji et al., 2005). However, as with securin, RNAi-mediated

restoration of cyclin B1 levels alone was not sufficient to abrogate mitotic delay. Only when simultaneous restoration of both securin and cyclin B1 was carried out were the mitotic effects of cyclin E deregulation neutralized. The contribution of two distinct and possibly synergistic mitotic inhibitors explains why seemingly modest elevation of levels of these proteins has a profound effect on progression through mitosis.

The nature of cyclin E-mediated mitotic delay.

Based on observations made from fixed cells, deregulation of cyclin E causes accumulation of cells either in a prometaphase-like state or a state where chromosomes are almost but not completely aligned on the metaphase plate. This categorization, however, was a formalism. Since these are static observations, we cannot describe the sequence of events in real-time that led to the accumulation of these cell types. It is possible that both of these phenotypes reflect the same population resulting from an inability to lose sister chromatid cohesion, as suggested above. Normally, centromeric cohesion is lost when bioriented chromosomes are aligned at metaphase. However, the inability to lose cohesion in a timely manner may promote an unusually dynamic situation where chromosomes under tension cyclically move toward and away from the metaphase plate, potentially accounting for both of the observed populations that accumulate as a result of cyclin E deregulation. Indeed, in time-lapse series of such cells, chromosomes appeared be unusually dynamic, undergoing significant oscillatory movements for long periods of time. However, because spindles and centromeres were not visible under these circumstances it was not possible to evaluate the attachment or tension status of chromosomes. The observation that mitotic chromosomes in cells deregulated for cyclin E expression appear hypercondensed (e.g. Fig. 1d) is also consistent with a prolonged prometaphase or metaphase due to inability to lose cohesion in a timely fashion (Gimenez-Abian et al., 2005a; Waizenegger et al., 2002).

Materials and Methods

Cell Culture and modeling cyclin E deregulation

Immortalized human fibroblasts (IHF) and immortalized mammary epithelial cells (IME), two cell lines immortalized by the stable transfection of the human telomerase reverse transcriptase gene (kind gift from J. Shay, The University of Texas Southwestern Medical Center, Dallas, TX), were used in initial experiments for chromosome painting, flow cytometry, and live-cell microscopy analysis. U2OS cells, an osteosarcoma cell line, were used for immunofluorescence and live-cell microscopy experiments. KB cells, a human nasopharyngeal epidermoid carcinoma and breast cancer-derived cell lines MDA-MB-157, -436, and -468 obtained from the American Type Culture Collection (Manassas, VA), were utilized for immunofluorescence microscopy and biochemical experiments. IME cells were cultured in MCDB media (Gibco) and supplemented with 1% FCS, H-Transferrin, EGF, BPE, and insulin, plus antibiotics. All others cells were grown in DMEM (Gibco BRL) supplemented with 10% FCS or 20% NCS and 100U/ml penicillin, 1.0 mg/ml streptomycin, and L-glutamine.

Recombinant retroviruses expressing a hyperstable form of cyclin E (T380A) or a control empty-vector were prepared using the 293T-derived packaging cell line Phoenix-Ampho and the pBABE retroviral plasmid vector (Morgenstern and Land, 1990) containing a hygromycin resistance marker for selection of long-term, stable expression mediated by the constitutive retrovirus LTR promoter. Concentrated retrovirus was added to cells with an equal amount of medium (10% FCS) for 24 hours, after which fresh media was added. Cells carrying the retrovirus construct were selected after 48 hours using 400ng/ml hygromycin.

Recombinant adenovirus expressing wild type (WT) cyclin E or a control empty-vector under the constitutive CMV promoter were purified by CsCl ultracentrifugation. Cells were transduced with approximately 1000 v.p./cell (comparable to levels used in (Ekholm-Reed et al., 2004a) in a low volume of medium with 0% serum for 2 hours, then additional medium plus 10% FCS was added for 24 hours.

Cyclin E expression in IME, U2OS, and KB cells was assayed by Western blot and immunofluorescence microscopy.

The histone H2B-GFP retrovirus was constructed from an H2B-GFP expression plasmid (BOS H2BGFP-N1, a gift from Kevin Sullivan, National University of Ireland, Galway Ireland) (Kanda et al., 1998). The H2B-GFP was cut and ligated into a pBabe backbone, containing a neomycin-resistance marker for selection.

SDS-PAGE electrophoresis and Western Blotting Analysis

Lysates were extracted in cold lysis buffer (50mM Tris, 150mM NaCL, 1mM EDTA, 1% Triton X-100 detergent, plus phosphatases and proteases), sonicated and spun down for 10 mins at 10,000g at 4°C, and protein concentrations were determined using Bradford solution (Bio Rad) read at 595nM. For Western Blotting analysis, samples were transferred onto Immobilon P membranes (Millipore) in Tris-glycine transfer buffer with 10% methanol. Primary antibody was added in 5% nonfat milk in 1X TBS plus 0.1% TritonX-100 (TBS-T = 10 mM Tris, 150 mM NaCl, 0.1% TritonX-100, pH 8) overnight at 4°C. Horseradish peroxidase-conjugated secondary antibodies (1:5000) diluted in 5% milk were incubate with the membrane for 1 hour at RT. Primary antibodies used were anti-cyclin E monoclonal antibody (HE12, Santa Cruz) 1:1000, anti-cyclin B1 monoclonal antibody (Pharmingen) 1:1000, anti-cyclin A polyclonal antibody (Santa Cruz) 1:1000, anti-Cdc20 polyclonal antibody (Abcam) 1:300, anti-Cdh1 monoclonal antibody (Calbiochem) 1:200, anti-Securin monoclonal antibody (Abcam) 1:200, anti-Myc (9E10) (Sigma), and anti-β-actin polyclonal antibody (Sigma) 1:10,000.

Immunofluorescence

Cells were plated onto acid-washed glass coverslips. Cells were fixed for 10 minutes at room temperature in 2% paraformaldehyde (PFA) in 1XPBS and 10 minutes in methanol at -20 degrees or cold methanol alone for 10 minutes (for detection of cyclin E). Cells were then permeabilized with PBS-TX

(1XPBS + 0.1% Triton X-100) for 15mins followed by incubation in blocking solution (PBS-TX + 1% BSA) at 37 degrees for 30 minutes. Coverslips were incubated with primary antibodies diluted in blocking solution overnight at 4 degrees in a humidity chamber. Secondary antibodies were used at a dilution of 1:250 (Cy2, Rhodamine Red-X, or Cy5 – Jackson Immunorearch Laboratories) and incubated for 1 hour at RT. Cells were washed and dehydrated with sequential washes of 70%, 90%, and 100% ethanol. Coverslips were mounted using SloFade with 4', 6- diamidino-2-phenylindole (DAPI) (Molecular Probes). Primary antibodies used were anti-cyclin E monoclonal antibody (HE12) 1:1000, anti-cyclin B1 monoclonal antibody (Pharmingen) 1:1000, anti-phosphorylated histone H3 (mitotic marker, Upstate) 1:400, anti-α tubulin (Dm1a, Sigma) 1:1000, anti-Sm human autosera (centromere-binding protein, gift from Kevin Sullivan, National University of Ireland, Galway Ireland) 1:100, and sheep polyclonal anti-BrdU (Research Diagnostics, Inc.).

Deconvolution Microscopy

Images were collected at intervals of 0.3 μm in the Z-direction on a DeltaVision wide field optical sectioning microscope system, based on an Olympus IX70 epifluorescence microscope (Applied Precision). A 60X or 100X (1.35 NA) neofluor oil immersion lens was used. Images were processed using a constrained iterative deconvolution algorithm. All images shown are projections of multiple focal planes, created using SoftWoRx analysis software (Applied Precision), and contain information from 3-dimensional image stacks.

Live-Cell Microscopy

IME or U2OS cells expressing H2B-GFP were grown directly on glass coverslips. Cells were maintained during imaging in phenol red-free Dulbecco's modified eagle medium plus 10 mM Hepes pH 7.5 buffer in a closed-chamber system (Bioptics) on a heated stage at 37°C. Five, 3μm-sections of DIC

and FITC fluorescence images were acquired at 1-minute intervals with a cooled charge couple device (CCD) camera mounted on a DeltaVision deconvolution microscope.

Flow Cytometry

For flow cytometry, cells were collected by trypsinization, washed with 1XPBS, and fixed with 70% ethanol (added dropwise with agitation) overnight at -20°C. Samples were then washed and resuspended in 1ml of PBS-TX plus RNAse solution (10 μg/ml) and propidium iodide (2 μg/ml) overnight at 4°C. For BrdU staining, cells were pulsed with 10μM BrdU for 20 minutes prior to collection as discussed above. Cells were treated with 1ml HCL + 0.5% TX for 30 minutes RT to denature DNA. The cell suspension was neutralized with 2ml of 0.1M Borax. Cells were washed with 1XPBS and resuspended in 50μl 1X PBS/1%BSA/0.5% Tween-20 and incubated in FITC-conjugated anti-BrdU antibody (2.5μg/ml) for 1 hour at RT. Cells were then washed and incubated with PI overnight as described above. Before analysis, cells were filtered through a 74μm mesh (Small Parts) to remove cell clumps before detection on a FACS Calibur II (Becton-Dickinson Immunocytometry Systems). For each cell line, 30,000 cells were counted/sample. Data were analyzed using CellQuest (Becton-Dickinson Immunocytometry Systems). All cell lines were analyzed using the same user-defined Gates and Regions to obtain percentages of cells with a G1, S, or G2/M DNA content.

Thymidine block-release protocol for synchronous release into mitosis

KB cells were transduced with EV-control or cyclin E adenovirus for 2 hours, then incubated in medium with 1.5mM thymidine overnight (~18hrs). Cells were released into S phase and through mitosis by adding 10% FCS medium (with or without 100nM nocodazole, as indicated), following three washes in warm medium. Cells were collected by trypsinization at various time points and split into samples for Western blot and flow cytometry.

siRNA transfections

Small interfering RNAs (21-mers) targeting and GFP, Cdh1, securin, and cyclin B (si*GENOME*, Dharmacon) were used to reduce protein expression in KB cells. Cells were transfected using Lipofectamine 2000 (12μl/10cm dish) (Invitrogen) with siRNA (10pM cyclin B1/securin-specific siRNA, 5nM Cdh1-specific siRNA, plus GFP-specific siRNA up to 20nM total siRNA concentration, or 20nM GFP-specific siRNA alone). Complexes were incubated for 20 mins at RT before adding to cells for 24 hours.

Immunoprecipitations and Kinase Assays

Cell lysates were subjected to immunoprecipitation followed by histone H1 kinase assay or Western blot. IME or KB cells were lysed in lysis buffer (50mM Tris, 150mM NaCL, 1mM EDTA, 1% Triton X-100 detergent, plus phosphatases and proteases) on ice. For kinase assays, anti-Cdk2 or IgG1 antibody (7.5 μg) was added to the lysates with gammabind G sepharose beads (100 μl of a 50% slurry, Pharmacia) for 2 hours at 4°C. Beads were washed 3-5 times with lysis buffer and 2 times with 1x reaction buffer (without ATP). Beads were resupended in 2x reaction buffer (40mM Tris-HCL, pH7.5, and 15mM MgCl2), 20μM ATP, 20μg histone H1, and 10μCi ATP-γ^{32}P and incubated for 30 minutes at 37°C. Samples were prepared and run on an 11% SDS-PAGE gel, and autoradiography was performed or phosphorylation was quantified using a phosphoimager.

Cdh1 kinase assays were performed as above with *E. coli* purified GST-Cdh1 (2 μg) as a substrate in the kinase reaction. GST peptide alone (10μg) and histone H1 (2μg) kinase assays were used to compared cyclin E/Cdk2 kinase activity.

GST purification of Cdh1 and expression of Myc-tagged Cdh1

GST-Cdh1-WT (a gift from Claus Sorensen, Danish Cancer Society, Institute of Cancer Biology, DK-2100 Copenhagen, Denmark) had been cloned into the GST-2TK plasmid (Pharmicia Upjohn). The fusion protein was expressed in *E.coli* bacteria after induction with IPTG, bound to glutathione-Sepharose, and eluted with reduced glutathione. The washes and eluted fractions were run on an SDS-PAGE gel and stained with Coomassie to evaluate purity. GST-Cdh1 was observed running at 75kD with degradation bands running below.

Myc-tagged Cdh1 constructs (WT, AAA, and 4A, or empty vector pX-myc) (gifts from Claus Sorensen, Danish Cancer Society, Institute of Cancer Biology, DK-2100 Copenhagen, Denmark), described in (Sorensen et al., 2001), were expressed in 293T cells along with purified cyclin E or cyclin A using calcium-phosphate transfections and collected following 48 hours of transfection. 9E10 anti-Myc antibody (Sigma) was used for immunoprecipitation. Beads were boiled in SDS-running buffer and analyzed by Western blot. Whole cell lysates and IPs were immunoblotted for cyclin E, cyclin A, or Cdh1.

Ubiquitylation assays

Ubiquitylation assays were performed using APC purified from 200µl of Xenopus extract following immunoprecipitation with anti-Cdc27 conjugated beads. Beads were washed 4 times in Xenopus buffer (500mM KCL, 0.5% NP-40) prior to use in the ubiquitylation assays. Cdh1, used to activate the APC, was in vitro translated in rabbit reticulocytes. A cold kinase assay was performed on Cdh1 prior to its addition to the APC ubiquitylation assay. In the kinase assay, Cdh1 was incubated in kinase buffer (Tris pH 7.5 1M 50mM 50, MgCl2, 1M 10mM 10, DTT 1M 2mM 2, ATP 200mM 200µM 1, Okadaic Acid 500µM 5µM, EGTA 0.5M 1mM) at 4 °C for 30min with purified cyclin E or cyclin A/Cdk2 to phosphorylate Cdh1. The kinase mix was removed and an aliquot was saved for analysis. Cdh1 was washed in Xenopus buffer and added to the ubiquitylation assay. Purified cyclin B1 was used as the substrated for the APC ubiquitylation assay.

For the ubiquitylation assay, 5µl of reaction cocktail (APC Reaction Cocktail: NRG 1X, E1 20ng/ l, E2-UbcH10 0.100µg/µl, E3-APC 1.25µg/µl, xenopus Cyclin B1 NT 10ul, and xenopus buffer - to 50ul total) was added with or without purified Cdh1 and incubated at RT with constant mixing. At time points, 0mins, 15mins, and 30mins, 1µl of reaction was removed and added to 5µl sample buffer to analyze by Western blot. Samples were run on a 14% gel, transferred, and exposed in a phosphorimager cassette.

Kinase reactions: 200uM Roscovitine inhibitor was added to 1µl Kinase Buffer as a control or to cyclin E and cyclin A/Cdk2 kinases and incubated at 30°C for 15mins. This was used to inhibit the kinase activity of cyclin E and cyclin A/Cdk2. Next, 2µl of in vitro translated Cdh1 or kinase buffer was added and incubated at 30°C for 1h. 0.2µl of the Roscovitine inhibitor was added to the remaining reactions to inhibit the residual kinase activity of Cdk2 and incubated another 15mins prior to addition of Cdh1 to the APC ubiquitylation assay. This was to ensure that Cdk2 was not phosphorylating the APC directly.

Acknowledgements

This work was supported by NIH grants CA78343 to SIR and JMK was supported by Department of Defense Predoctoral Fellowship DAMD17-03-1-0383.

Arata, Y., M. Fujita, K. Ohtani, S. Kijima, and J.Y. Kato. 2000. Cdk2-dependent and -independent pathways in E2F-mediated S phase induction. *J Biol Chem*. 275:6337-45.

Blanco, M.A., A. Sanchez-Diaz, J.M. de Prada, and S. Moreno. 2000. APC(ste9/srw1) promotes degradation of mitotic cyclins in G(1) and is inhibited by cdc2 phosphorylation. *Embo J*. 19:3945-55.

Bortner, D.M., and M.P. Rosenberg. 1997. Induction of Mammary Gland Hyperplasia and Carcinomas in Transgenic Mice Expressing Human Cyclin E. *Mol. and Cell. Biol.* 17:453-459.

Brandeis, M., and T. Hunt. 1996. The proteolysis of mitotic cyclins in mammalian cells persists from the end of mitosis until the onset of S phase. *Embo J*. 15:5280-9.

Clurman, B.E., R.J. Sheaff, K. Thress, M. Groudine, and J.M. Roberts. 1996. Turnover of cyclin E by the ubiquitin-proteasome pathway is regulated by cdk2 binding and cyclin phosphorylation. *Genes Dev*. 10:1979-90.

Cohen-Fix, O., J.M. Peters, M.W. Kirschner, and D. Koshland. 1996. Anaphase initiation in Saccharomyces cerevisiae is controlled by the APC-dependent degradation of the anaphase inhibitor Pds1p. *Genes Dev*. 10:3081-93.

Dulic, v., E. Lees, and S. Reed. 1992. Association of human cyclin E with a periodic G1/S phase protein kinase. *Science*. 257:1958-61.

Dutta, A., R. Chandra, L.M. Leiter, and S. Lester. 1995. Cyclins as markers of tumor proliferation: Immunocytochemical studies in breast cancer. *Proc. Natl. Acad. Sci. USA*. 92:5386-5390.

Ekholm-Reed, S., J. Mendez, D. Tedesco, A. Zetterberg, B. Stillman, and S.I. Reed. 2004a. Deregulation of cyclin E in human cells interferes with prereplication complex assembly. *J Cell Biol*. 165:789-800.

Ekholm-Reed, S., C.H. Spruck, O. Sangfelt, F. van Drogen, E. Mueller-Holzner, M. Widschwendter, A. Zetterberg, and S.I. Reed. 2004b. Mutation of hCDC4 leads to cell cycle deregulation of cyclin E in cancer. *Cancer Res*. 64:795-800.

Ekholm, S.V., and S.I. Reed. 2000. Regulation of G(1) cyclin-dependent kinases in the mammalian cell cycle. *Curr Opin Cell Biol*. 12:676-84.

Erlandsson, F., C. Wahlby, S. Ekholm-Reed, A.C. Hellstrom, E. Bengtsson, and A. Zetterberg. 2003. Abnormal expression pattern of cyclin E in tumour cells. *Int J Cancer*. 104:369-75.

Erlanson, M., and G. Landberg. 2001. Prognostic implications of p27 and cyclin E protein contents in malignant lymphomas. *Leuk Lymphoma*. 40:461-70.

Fang, G., H. Yu, and M.W. Kirschner. 1998. Direct binding of CDC20 protein family members activates the anaphase-promoting complex in mitosis and G1. *Mol Cell*. 2:163-71.

Geng, Y., Q. Yu, E. Sicinska, M. Das, J.E. Schneider, S. Bhattacharya, W.M. Rideout, R.T. Bronson, H. Gardner, and P. Sicinski. 2003. Cyclin E ablation in the mouse. *Cell*. 114:431-43.

Gimenez-Abian, J.F., L.A. Diaz-Martinez, I.C. Waizenegger, G. Gimenez-Martin, and D.J. Clarke. 2005a. Separase is required at multiple pre-anaphase cell cycle stages in human cells. *Cell Cycle*. 4:1576-84.

Gimenez-Abian, J.F., L.A. Diaz-Martinez, K.G. Wirth, C.A. Andrews, G. Gimenez-Martin, and D.J. Clarke. 2005b. Regulated separation of sister centromeres depends on the spindle assembly checkpoint but not on the Anaphase Promoting Complex/Cyclosome. *Cell Cycle*. 4:1561-75.

Gorr, I.H., D. Boos, and O. Stemmann. 2005. Mutual inhibition of separase and Cdk1 by two-step complex formation. *Mol Cell*. 19:135-41.

Harbour, J.W., R.X. Luo, A. Dei Santi, A.A. Postigo, and D.C. Dean. 1999. Cdk phosphorylation triggers sequential intramolecular interactions that progressively block Rb functions as cells move through G1. *Cell*. 98:859-69.

Hauf, S., I.C. Waizenegger, and J.M. Peters. 2001. Cohesin cleavage by separase required for anaphase and cytokinesis in human cells. *Science*. 293:1320-3.

Hendzel, M.J., Y. Wei, M.A. Mancini, A. Van Hooser, T. Ranalli, B.R. Brinkley, D.P. Bazett-Jones, and C.D. Allis. 1997. Mitosis-specific phosphorylation of histone H3 initiates primarily within pericentromeric heterochromatin during G2 and spreads in an ordered fashion coincident with mitotic chromosome condensation. *Chromosoma*. 106:348-60.

Hubalek, M.M., A. Widschwendter, M. Erdel, A. Gschwendtner, H.M. Fiegl, H.M. Muller, G. Goebel, E. Mueller-Holzner, C. Marth, C.H. Spruck, S.I. Reed, and M. Widschwendter. 2004. Cyclin E dysregulation and chromosomal instability in endometrial cancer. *Oncogene*. 23:4187-92.

Jaspersen, S.L., J.F. Charles, and D.O. Morgan. 1999. Inhibitory phosphorylation of the APC regulator Hct1 is controlled by the kinase Cdc28 and the phosphatase Cdc14. *Curr Biol*. 9:227-36.

Ji, J.Y., J. Crest, and G. Schubiger. 2005. Genetic interactions between Cdk1-CyclinB and the Separase complex in Drosophila. *Development*. 132:1875-84.

Kanda, T., K.F. Sullivan, and G.M. Wahl. 1998. Histone-GFP fusion protein enables sensitive analysis of chromosome dynamics in living mammalian cells. *Curr Biol*. 8:377-85.

Keyomarsi, K., D. Conte, Jr., W. Toyofuku, and M.P. Fox. 1995. Deregulation of cyclin E in breast cancer. *Oncogene*. 11:941-50.

Keyomarsi, K., S.L. Tucker, T.A. Buchholz, M. Callister, Y. Ding, G.N. Hortobagyi, I. Bedrosian, C. Knickerbocker, W. Toyofuku, M. Lowe, T.W. Herliczek, and S.S. Bacus. 2002. Cyclin E and survival in patients with breast cancer. *N Engl J Med*. 347:1566-75.

Knoblich, J.A., K. Sauer, L. Jones, H. Richardson, R. Saint, and C.F. Lehner. 1994. Cyclin E controls S phase progression and its down-regulation during Drosophila embryogenesis is required for the arrest of cell proliferation. *Cell*. 77:107-20.

Koff, A., F. Cross, J. Schumacher, K. Philippe, and J. Roberts. 1991. Human cyclin E, a newe cyclin that interacts with two members of the CDC2 family. *Cell*. 66:1217.

Kramer, E.R., N. Scheuringer, A.V. Podtelejnikov, M. Mann, and J.M. Peters. 2000. Mitotic regulation of the APC activator proteins CDC20 and CDH1. *Mol Biol Cell*. 11:1555-69.

Lukas, C., C.S. Sorensen, E. Kramer, E. Santoni-Rugiu, C. Lindeneg, J.M. Peters, J. Bartek, and J. Lukas. 1999. Accumulation of cyclin B1 requires E2F and cyclin-A-dependent rearrangement of the anaphase-promoting complex. *Nature*. 401:815-8.

Lukas, J., T. Herzinger, K. Hansen, M.C. Moroni, D. Resnitzky, K. Helin, S.I. Reed, and J. Bartek. 1997. Cycline E-induced S phase without activation of the pRb/E2F pathway. *Genes Dev.* 11:1479-1492.

Mailand, N., and J.F. Diffley. 2005. CDKs promote DNA replication origin licensing in human cells by protecting Cdc6 from APC/C-dependent proteolysis. *Cell*. 122:915-26.

Morgenstern, J.P., and H. Land. 1990. Advanced mammalian gene transfer: high titre retroviral vectors with multiple drug selection markers and a complementary helper-free packaging cell line. *Nucleic Acids Res*. 18:3587-96.

Nielsen, N.H., C. Arnerlov, S. Cajander, and G. Landberg. 1998. Cyclin E expression and proliferation in breast cancer. *Anal Cell Pathol*. 17:177-88.

Ohtsubo, M., and J.M. Roberts. 1993. Cyclin-dependent regulation of G1 in mammalian fibroblasts. *Science*. 259:1908-12.

Ohtsubo, M., A.M. Theodoras, J. Schumacher, J.M. Roberts, and M. Pagano. 1995. Human cyclin E, a nuclear protein essential for the G1-to-S phase transition. *Mol Cell Biol*. 15:2612-24.

Porter, P.L., K.E. Malone, P.J. Heagerty, G.M. Alexander, L.A. Gatti, E.J. Firpo, J.R. Daling, and J.M. Roberts. 1997. Expression of cell-cycle regulators p27Kip1 and cyclin E, alone and in combination, correlate with survival in young breast cancer patients. *Nat Med*. 3:222-5.

Rajagopalan, H., P.V. Jallepalli, C. Rago, V.E. Velculescu, K.W. Kinzler, B. Vogelstein, and C. Lengauer. 2004. Inactivation of hCDC4 can cause chromosomal instability. *Nature*. 428:77-81.

Rasband, W.S. 2005. ImageJ. *U. S. National Institutes of Health, Bethesda,*

Maryland, USA. http://rsb.info.nih.gov/ij/,.
Resnitzky, D., M. Gossen, H. Bujard, and S.I. Reed. 1994. Acceleration of the G1/S phase transition by expression of cyclins D1 and E with an inducible system. *Mol Cell Biol*. 14:1669-79.
Salah, S.M., and K. Nasmyth. 2000. Destruction of the securin Pds1p occurs at the onset of anaphase during both meiotic divisions in yeast. *Chromosoma*. 109:27-34.
Sandhu, C., and J. Slingerland. 2000. Deregulation of the cell cycle in cancer. *Cancer Detect Prev*. 24:107-18.
Sauer, K., and C.F. Lehner. 1995. The role of cyclin E in the regulation of entry into S phase. *Prog Cell Cycle Res*. 1:125-39.
Sigrist, S., H. Jacobs, R. Stratmann, and C.F. Lehner. 1995. Exit from mitosis is regulated by Drosophila fizzy and the sequential destruction of cyclins A, B and B3. *Embo J*. 14:4827-38.
Sigrist, S.J., and C.F. Lehner. 1997. Drosophila fizzy-related down-regulates mitotic cyclins and is required for cell proliferation arrest and entry into endocycles. *Cell*. 90:671-81.
Smith, A.P., M. Henze, J.A. Lee, K.G. Osborn, J.M. Keck, D. Tedesco, D.M. Bortner, M.P. Rosenberg, and S.I. Reed. 2006. Deregulated cyclin E promotes p53 loss of heterozygosity and tumorigenesis in the mouse mammary gland. *Oncogene*.
Sorensen, C.S., C. Lukas, E.R. Kramer, J.M. Peters, J. Bartek, and J. Lukas. 2000. Nonperiodic activity of the human anaphase-promoting complex-Cdh1 ubiquitin ligase results in continuous DNA synthesis uncoupled from mitosis. *Mol Cell Biol*. 20:7613-23.
Sorensen, C.S., C. Lukas, E.R. Kramer, J.M. Peters, J. Bartek, and J. Lukas. 2001. A conserved cyclin-binding domain determines functional interplay between anaphase-promoting complex-Cdh1 and cyclin A-Cdk2 during cell cycle progression. *Mol Cell Biol*. 21:3692-703.
Spruck, C.H., H. Strohmaier, O. Sangfelt, H.M. Muller, M. Hubalek, E. Muller-Holzner, C. Marth, M. Widschwendter, and S.I. Reed. 2002. hCDC4 gene mutations in endometrial cancer. *Cancer Res*. 62:4535-9.
Spruck, C.H., K.-A. Won, and S.I. Reed. 1999. Deregulated cyclin E induces chromosome instability. *Science*. 401:297-300.
Strohmaier, H., C.H. Spruck, P. Kaiser, K.-A. Won, O. Sangfelt, and S.I. Reed. 2001. Human F-box protein hCdc4 targets cyclin E for proteolysis and is mutated in a breast cancer cell line. *Nature*. 413:316-322.
Thiagalingam, S., S. Laken, J.K.V. Willson, S.D. Markowitz, K.W. Kinzler, B. Bogelstein, and C. Lengauer. 2000. Mechanisms underlying losses of heterozygosity in human colorectal cancers. *Proc. Natl. Acad. Sci. USA*. 98:2698-2702.
Uhlmann, F., F. Lottspeich, and K. Nasmyth. 1999. Sister-chromatid separation at anaphase onset is promoted by cleavage of the cohesin subunit Scc1. *Nature*. 400:37-42.
Uhlmann, F., D. Wernic, M.A. Poupart, E.V. Koonin, and K. Nasmyth. 2000. Cleavage of cohesin by the CD clan protease separin triggers anaphase in yeast. *Cell*. 103:375-86.
Visintin, R., S. Prinz, and A. Amon. 1997. CDC20 and CDH1: a family of substrate-specific activators of APC-dependent proteolysis. *Science*. 278:460-3.
Waizenegger, I., J.F. Gimenez-Abian, D. Wernic, and J.M. Peters. 2002. Regulation of human separase by securin binding and autocleavage. *Curr Biol*. 12:1368-78.
Waizenegger, I.C., S. Hauf, A. Meinke, and J.M. Peters. 2000. Two distinct pathways remove mammalian cohesin from chromosome arms in prophase and from centromeres in anaphase. *Cell*. 103:399-410.
Won, K.A., and S.I. Reed. 1996. Activation of cyclin E/CDK2 is coupled to site-specific autophosphorylation and ubiquitin-dependent degradation of cyclin E. *Embo J*. 15:4182-93.
Ye, X., G. Nalepa, M. Welcker, B.M. Kessler, E. Spooner, J. Qin, S.J. Elledge, B.E. Clurman, and J.W. Harper. 2004. Recognition of phosphodegron motifs in human cyclin E by the SCF(Fbw7) ubiquitin ligase. *J Biol Chem*. 279:50110-9.

Zachariae, W., M. Schwab, K. Nasmyth, and W. Seufert. 1998. Control of cyclin ubiquitination by CDK-regulated binding of Hct1 to the anaphase promoting complex. *Science*. 282:1721-4.

Zhang, H.S., A.A. Postigo, and D.C. Dean. 1999. Active transcriptional repression by the Rb-E2F complex mediates G1 arrest triggered by p16INK4a, TGFbeta, and contact inhibition. *Cell*. 97:53-61.

Zou, H., T.J. McGarry, T. Bernal, and M.W. Kirschner. 1999. Identification of a vertebrate sister-chromatid separation inhibitor involved in transformation and tumorigenesis. *Science*. 285:418-22.

Zur, A., and M. Brandeis. 2001. Securin degradation is mediated by fzy and fzr, and is required for complete chromatid separation but not for cytokinesis. *Embo J*. 20:792-801.